DFVLR

Deutsche Forschungs- und
Versuchsanstalt
für Luft- und Raumfahrt

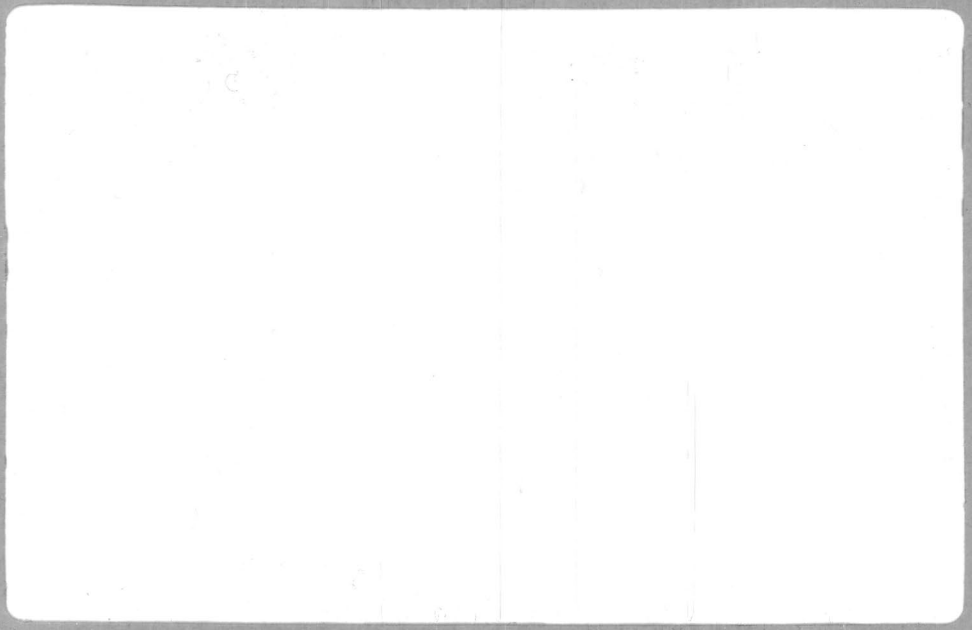

Interner Bericht

IB 152-80/12

Initital Postbuckling Behaviour of Orthotropic Shells

B. Geier

Paper presented at the
12th ICAS Congress
Munich October 12-17, 1980

DFVLR, Institut für Strukturmechanik, D-3000 Braunschweig

1. Introduction

The research work reported in this paper was started following a series of buckling tests performed with curved orthotropic sandwich panels. Comparison of the test results with computed bifurcation buckling loads was very satisfactory. However, the tests also showed that the computed buckling loads normally are not sufficient for estimating the load carrying capacity of the panels. Some knowledge about the postbuckling behaviour of the panels was supported to be needed, too [1].

The calculation of the postbuckling behaviour requires the solution of non-linear boundary value problems and is laborious even with to-day's computers. However, if we are contented with an information on the behaviour in the very initial postbuckling range, the expenditure may be reduced considerably. A theory of the initial postbuckling behaviour of elastic structures was developed by W.T. KOITER [2] in 1945. An English translation was published in 1967. Alternative formulations of KOITER's theory were presented by P. SEIDE [3] and by B. BUDIANSKY [4].

The theory was applied to the buckling of compressed curved panels by W.T. KOITER [5] and to curved sandwich panels by G.G. POPE [6]. Their solutions were confined to panels long enough for buckling modes with several longitudinal waves. Moreover, they were generated for idealized boundary conditions which are not so representative of realistic structures. The treatment of more realistic boundary conditions has become feasible only with the modern high-speed computers.

The approach described in this paper is based on the computer program BEOS (Buckling of Eccentrically Orthotropic Sandwich Shells) [7] that was used to compute the buckling loads of the tested panels. As this program was designed to compute also vibration modes and frequencies [8] it admits the computation of several eigenmodes and eigenvalues. Hence, higher buckling modes together with the corresponding bifurcation loads can be computed. It was decided, therefore, to base the analysis of the initial postbuckling behaviour on expansions of the required

functions into series' of buckling modes. For calculating certain energy integrals the method used in the program BEOS was properly extended. Thus the calculation of the initial postbuckling behaviour of shallow panels could be programmed as an appendix to that computer code. All the shell configurations to which BEOS may be applied, can now be analysed whith respect to their initial postbuckling behaviour. The most general configuration is a skew sandwich shell with orthotropic core and dissimilar orthotropic faces the thicknesses of which may be of the order of the core height. A variety of boundary conditions may be treated, and there is practically no restriction concerning the in-plane loads.

This paper summarizes, in its first part, the analytical foundations of the solution method. Essentially it is based on the presentation of B. BUDIANSKY [4]. In order to achieve a certain degree of self-consistancy some of his arguments and results had to be reproduced. Having established general formulae for the quantities characterizing the initial postbuckling behaviour, it is outlined in the report how these relations can be evaluated numerically following a buckling analysis. A presentation of results follows, with special emphasis on the tested panels relating the results of the computation to their measured behaviour.

2. Analysis of Equilibrium States

2.1 Potential Energy of the Shell

In order to desrcibe completely the deformation of a shallow sandwich shell the theoretical model of ref. [1] uses five quantities, all of them functions of the coordinates x,y which span the reference surface of the shell: The two "in-plane" deflections u and v, the normal deflection w, and the transverse shear strains β , γ of the sandwich core, see. Fig. 1. For brevity of notation these quantities are assembled in a "displacement" vector $\mathbf{u}$:

$$\mathbf{u}^T = [w, u, v, \beta, \gamma] = [u^1, u^2, u^3, u^4, u^5] \tag{2.1}$$

A deformation of the shell, as opposed to a rigid body displacement, is characterised by any non-vanishing components of the vector of generalised strains $\boldsymbol{\varepsilon}(\mathbf{u})$. The components of this vector are the "in-plane" normal and shear strains of the reference surface, the changes of curvature of the reference surface, the shear strain of the core, and three more quantitites the physical meaning of which is not so obvious. They are needed to account for the fact that the faces of the sandwich are allowed to be of different thickness which is not negligably small compared to the height of the core.

The strain components are linear functions of the displacements except the "in-plane" strains, which have non-linear parts. The special form of these non-linear components suggests to split the strain vector into a linear and a nonlinear part in the following way:

$$\boldsymbol{\varepsilon}(\mathbf{u}) = \boldsymbol{\varepsilon}^{L}(\mathbf{u}) + \frac{1}{2}\,\boldsymbol{\varepsilon}^{N}(\mathbf{u},\mathbf{u}). \tag{2.2}$$

The nonlinear part $\boldsymbol{\varepsilon}^{N}(\mathbf{u},\mathbf{u})$ may be considered as the special case of a symmetric bilinear operator $\boldsymbol{\varepsilon}^{N}(\mathbf{u},\mathbf{v})$ with the properties

$$\begin{aligned} &\boldsymbol{\varepsilon}^{N}(\mathbf{u},\mathbf{v}) = \boldsymbol{\varepsilon}^{N}(\mathbf{v},\mathbf{u}), \\ &\boldsymbol{\varepsilon}^{N}(\mathbf{u},\mathbf{v}+\mathbf{w}) = \boldsymbol{\varepsilon}^{N}(\mathbf{u},\mathbf{v}) + \boldsymbol{\varepsilon}^{N}(\mathbf{u},\mathbf{w}). \end{aligned} \tag{2.3}$$

Only the first three components of this vector are non-zero.

The relations appearing somewhat abstract in the paragraphs above, will become more familiar if written down in their full lengths:

$$(2.4)\quad \boldsymbol{\varepsilon}^L(\mathbf{u}) = \begin{Bmatrix} \frac{\partial u}{\partial x} - \frac{w}{r_x} \\ \frac{\partial v}{\partial y} - \frac{w}{r_y} \\ \frac{\partial u}{\partial y} + \frac{\partial v}{\partial x} \\ \frac{\partial^2 w}{\partial x^2} \\ \frac{\partial^2 w}{\partial y^2} \\ 2\frac{\partial^2 w}{\partial x \partial y} \\ \frac{\partial \beta}{\partial x} \\ \frac{\partial \gamma}{\partial y} \\ \frac{\partial \beta}{\partial y} + \frac{\partial \gamma}{\partial x} \\ \beta \\ \gamma \end{Bmatrix}, \quad \boldsymbol{\varepsilon}^N(\mathbf{u}_1, \mathbf{u}_2) = \begin{Bmatrix} \frac{\partial w_1}{\partial x}\frac{\partial w_2}{\partial x} \\ \frac{\partial w_1}{\partial y}\frac{\partial w_2}{\partial y} \\ \frac{\partial w_1}{\partial x}\frac{\partial w_2}{\partial y} + \frac{\partial w_1}{\partial y}\frac{\partial w_2}{\partial x} \\ 0 \\ 0 \\ 0 \\ 0 \\ 0 \\ 0 \\ 0 \\ 0 \\ 0 \end{Bmatrix}.$$

For $\boldsymbol{\varepsilon}^N(\mathbf{u}_1, \mathbf{u}_2)$ we get the usual relation of the nonlinear plate and shallow shell theory, if we substitute $\mathbf{u}_1 = \mathbf{u}_2 = \mathbf{u}$.

The total potential energy of the shell can now be written as

$$(2.5)\quad \Pi = \frac{1}{2}\int_{(A)} \boldsymbol{\varepsilon}(\mathbf{u})^T \mathbf{C}\, \boldsymbol{\varepsilon}(\mathbf{u})\, dA - \int_{(A)} \mathbf{p}^T \mathbf{u}\, dA - \int_{(S_N)} \tilde{\mathbf{N}}_0^T \mathbf{u}\, dS,$$

where $\mathbf{C}$ is the symmetric matrix of the constitutive law of the sandwich shell, the components of $\mathbf{p}$ are external surface forces and $\tilde{\mathbf{N}}_0$ comprises external in-plane forces acting upon the part S_N

of the edges.

In addition to the simplifying assumptions that have led to the above formulae we assume that in the basic prebuckling equilibrium state with displacements $\mathbf{u} = \hat{\mathbf{u}}$ the nonlinear part of the strain vector vanishes:

$$\boldsymbol{\varepsilon}^N(\hat{\mathbf{u}}, \mathbf{v}) = \mathbf{0} \ . \tag{2.6}$$

In the following part of this paper we shall consider equilibrium states deviating only slightly from a fundamental prebuckling state. We disregard the influence of external surface forces, and we assume the components of the vector of external edge loads to increase or decrease proportionally. Thus we write

$$\mathbf{u} = \hat{\mathbf{u}} + \mathbf{u}^* \quad ; \quad \mathbf{p} = \mathbf{0} \ ; \quad \tilde{\mathbf{N}}_0 = \lambda \mathbf{N}_0 \ . \tag{2.7}$$

Utilizing equs. (2.2) and (2.6) we get

$$\begin{aligned} \boldsymbol{\varepsilon}(\mathbf{u}) &= \boldsymbol{\varepsilon}^L(\hat{\mathbf{u}} + \mathbf{u}^*) + \frac{1}{2}\,\boldsymbol{\varepsilon}^N(\hat{\mathbf{u}} + \mathbf{u}^*, \hat{\mathbf{u}} + \mathbf{u}^*) \\ &= \boldsymbol{\varepsilon}^L(\hat{\mathbf{u}}) + \boldsymbol{\varepsilon}^L(\mathbf{u}^*) + \frac{1}{2}\,\boldsymbol{\varepsilon}(\mathbf{u}^*, \mathbf{u}^*) \ , \end{aligned}$$

and from equ. (2.5) the potential energy follows to be

$$\begin{aligned} \Pi = {} & \frac{1}{2}\int_{(A)} \boldsymbol{\varepsilon}^L(\hat{\mathbf{u}})^T \mathbf{C}\, \boldsymbol{\varepsilon}^L(\hat{\mathbf{u}})\, dA + \int_{(A)} \boldsymbol{\varepsilon}^L(\hat{\mathbf{u}})^T \mathbf{C}\, \boldsymbol{\varepsilon}^L(\mathbf{u}^*)\, dA \\ & + \frac{1}{2}\int_{(A)} \boldsymbol{\varepsilon}^L(\mathbf{u}^*)^T \mathbf{C}\, \boldsymbol{\varepsilon}^L(\mathbf{u}^*)\, dA + \frac{1}{2}\int_{(A)} \boldsymbol{\varepsilon}^L(\hat{\mathbf{u}})^T \mathbf{C}\, \boldsymbol{\varepsilon}^N(\mathbf{u}^*, \mathbf{u}^*)\, dA \\ & + \frac{1}{2}\int_{(A)} \boldsymbol{\varepsilon}^L(\mathbf{u}^*)^T \mathbf{C}\, \boldsymbol{\varepsilon}^N(\mathbf{u}^*, \mathbf{u}^*)\, dA + \frac{1}{8}\int_{(A)} \boldsymbol{\varepsilon}^N(\mathbf{u}^*, \mathbf{u}^*)^T \mathbf{C}\, \boldsymbol{\varepsilon}^N(\mathbf{u}^*, \mathbf{u}^*)\, dA \\ & - \lambda \int_{(S_N)} \mathbf{N}_0^T(\hat{\mathbf{u}} + \mathbf{u}^*)\, dS \ . \end{aligned} \tag{2.8}$$

Now

$$\hat{\Pi} = \frac{1}{2}\int_{(A)} \boldsymbol{\varepsilon}^L(\hat{\mathbf{u}})^T \mathbf{C}\, \boldsymbol{\varepsilon}^L(\hat{\mathbf{u}})\, dA - \lambda \int_{(S_N)} \mathbf{N}_0^T \hat{\mathbf{u}}\, dS \tag{2.9}$$

is the potential energy of the fundamental state. The expression

$$(2.10) \qquad \Pi^* = \int_{(A)} \boldsymbol{\varepsilon}^L(\hat{\mathbf{u}})^T \mathbf{C}\, \boldsymbol{\varepsilon}^L(\mathbf{u}^*)\, dA - \lambda \int_{(S_N)} \mathbf{N}_0^T \mathbf{u}^*\, dS = 0$$

is proportional to its first variation, and vanishes because the fundamental state is in equilibrium.

The internal forces in the fundamental state are

$$\hat{\mathbf{N}} = \mathbf{C}\, \boldsymbol{\varepsilon}^L(\hat{\mathbf{u}}) \ .$$

Since the relation is linear, we may as well write

$$(2.11) \qquad -\lambda \mathbf{N} = \mathbf{C}\, \boldsymbol{\varepsilon}^L(\hat{\mathbf{u}})$$

where $\mathbf{N}$ is a basic membrane force distribution. The negative sign has been chosen to get positive values for λ at compressive loads.

With equs. (2.9) through (2.11) equ. (2.8) simplifies to

$$(2.12) \qquad \Pi = \hat{\Pi} + \frac{1}{2} \int_{(A)} [\boldsymbol{\varepsilon}^L(\mathbf{u}^*)^T \mathbf{C}\, \boldsymbol{\varepsilon}^L(\mathbf{u}^*) - \lambda \mathbf{N} \boldsymbol{\varepsilon}^N(\mathbf{u}^*, \mathbf{u}^*)]\, dA$$

$$+ \frac{1}{2} \int_{(A)} \boldsymbol{\varepsilon}^L(\mathbf{u}^*)^T \mathbf{C}\, \boldsymbol{\varepsilon}^N(\mathbf{u}^*, \mathbf{u}^*)\, dA + \frac{1}{8} \int_{(A)} \boldsymbol{\varepsilon}^N(\mathbf{u}^*, \mathbf{u}^*)^T \mathbf{C}\, \boldsymbol{\varepsilon}^N(\mathbf{u}^*, \mathbf{u}^*)\, dA \ .$$

2.2 Equilibrium States Bifurcating from the Fundamental Path

2.2.1 Equilibrium Condition

With equ. (2.10) we have already formulated the equilibrium condition for the fundamental state, and we assume that we have a method to evaluate it. We now want to look for bifurcating equilibrium paths.

To find the equilibrium condition for bifurcating states we have to form the variation of the potential energy (2.12). The quantities to be varied are the displacements $\mathbf{u}^*$. We get

$$\delta\Pi = \int_{(A)} [\boldsymbol{\varepsilon}^L(\mathbf{u}^*)^T \mathbf{C}\, \boldsymbol{\varepsilon}^L(\delta\mathbf{u}) - \lambda \mathbf{N}^T \boldsymbol{\varepsilon}^N(\mathbf{u}^*, \delta\mathbf{u})]\, dA$$

$$+ \int_{(A)} \boldsymbol{\varepsilon}^L(\mathbf{u}^*)^T \mathbf{C}\, \boldsymbol{\varepsilon}^N(\mathbf{u}^*, \delta\mathbf{u})\, dA + \frac{1}{2} \int_{(A)} \boldsymbol{\varepsilon}^N(\mathbf{u}^*, \mathbf{u}^*)^T \mathbf{C}\, \boldsymbol{\varepsilon}^L(\delta\mathbf{u})\, dA \tag{2.13}$$

$$+ \frac{1}{2} \int_{(A)} \boldsymbol{\varepsilon}^N(\mathbf{u}^*, \mathbf{u}^*)^T \mathbf{C}\, \boldsymbol{\varepsilon}^N(\mathbf{u}^*, \delta\mathbf{u})\, dA \,.$$

2.2.2 Bifurcation Points

The integrands in equ. (2.13) are linear, quadratic, or of third order in $\mathbf{u}^*$. Near the bifurcation point the displacements $\mathbf{u}^*$ are very small. Therefore, the dominating part in the equilibrium condition is the linear one. Thus the solution properties at the bifurcation point, and in its close vicinity, may be evaluated from the variational equation.

$$\int [\boldsymbol{\varepsilon}^L(\mathbf{u}^*)^T \mathbf{C}\, \boldsymbol{\varepsilon}^L(\delta\mathbf{u}) - \lambda \mathbf{N}^T \boldsymbol{\varepsilon}^N(\mathbf{u}^*, \delta\mathbf{u})]\, dA = 0 \tag{2.14}$$

It constitutes an eigenvalue problem for determining the eigenvalues $\lambda = \lambda_i$ and the eigenmodes $\mathbf{u}^* = \mathbf{u}_i$.

The eigenmodes $\mathbf{u}_i$ are undetermined in their magnitude. They will be normalised to yield

$$\int \boldsymbol{\varepsilon}^L(\mathbf{u}_i)^T \mathbf{C}\, \boldsymbol{\varepsilon}^L(\mathbf{u}_i)\, dA = F \tag{2.15}$$

where F is a quantity of the correct dimension "work". It follows then from equ. (2.14) that

$$\int_{(A)} \mathbf{N}^T \boldsymbol{\varepsilon}^N(\mathbf{u}_i, \mathbf{u}_i)\, dA = \frac{F}{\lambda_i} \tag{2.16}$$

Moreover, it can be shown that between different eigenmodes the orthogonality relations

$$(2.17)\qquad \left.\begin{aligned} &\int_{(A)} \boldsymbol{\varepsilon}^L(\mathbf{u}_i)^T \mathbf{C}\, \boldsymbol{\varepsilon}^L(\mathbf{u}_k)\, dA = 0 \\ &\int_{(A)} \mathbf{N}^T \boldsymbol{\varepsilon}^N(\mathbf{u}_i, \mathbf{u}_k)\, dA = 0 \end{aligned}\right\} \; i \neq k$$

are valid.

2.3.3 Initial Postbuckling Behaviour

The first eigenvalue λ_1 corresponds to the buckling load of the shell. We shall assume that the corresponding eigenmode $\mathbf{u}_1$ is unique. Clearly the eigenmode $\mathbf{u}_1$ indicates the deformation pattern of the shell immediately after buckling. To trace the solution further into the postbuckling range a perturbation method is applied. We assume

$$(2.18)\qquad \begin{aligned} \mathbf{u}^* &= \zeta \mathbf{u}_1 + \zeta^2 \mathbf{v}_2 + \zeta^3 \mathbf{v}_3 + \dots \\ \lambda &= \lambda_1 + \alpha_1 \zeta + \alpha_2 \zeta^2 + \dots \quad . \end{aligned}$$

In this formulae the quantity ζ is a small parameter indicating the "content" of buckling mode in the deformation pattern. The coefficients α_1, α_2 show whether the shell continues to carry additional loads along the postbuckling path or not. This is illustrated in the following figures:

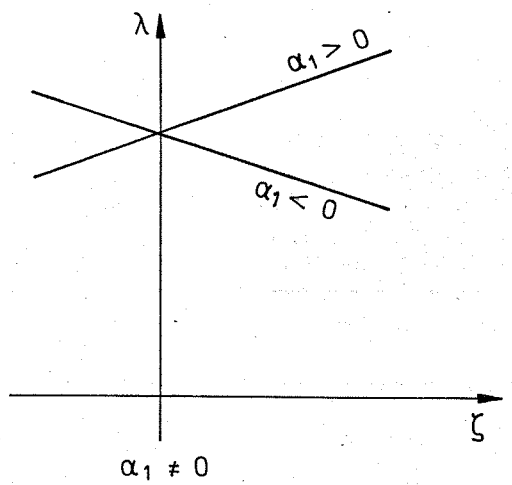

$\alpha_1 \neq 0$

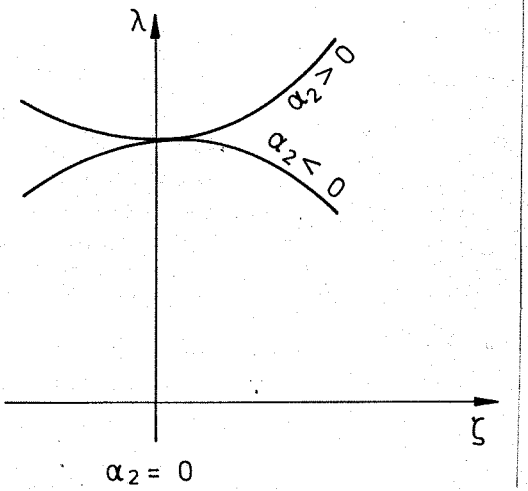

$\alpha_2 = 0$

The displacements $\mathbf{v}_2$, $\mathbf{v}_3$ in the expansion for $\mathbf{u}^*$ are supposed to be orthogonal to $\mathbf{u}_1$ in the sense that

$$\int_{(A)} \boldsymbol{\varepsilon}^L(\mathbf{u}_1)^T \mathbf{C}\, \boldsymbol{\varepsilon}^L(\mathbf{v}_i)\, dA = 0$$

(2.19)

$$\int_{(A)} \mathbf{N}^T \boldsymbol{\varepsilon}^N(\mathbf{u}_1, \mathbf{v}_i)\, dA = 0 \quad .$$

We proceed now by substituting the pertubation equations (2.18) into the equilibrium condition (2.13) and assemble equal powers of the pertubation factor ζ :

$$\begin{aligned}
\delta \Pi = {} & \zeta \Big\{ \int_{(A)} [\boldsymbol{\varepsilon}^L(\mathbf{u}_1)^T \mathbf{C} \boldsymbol{\varepsilon}^L(\delta\mathbf{u}) - \lambda_1 \mathbf{N}^T \boldsymbol{\varepsilon}^N(\mathbf{u}_1, \delta\mathbf{u})]\, dA \Big\} \\
& + \zeta^2 \Big\{ \int_{(A)} [\boldsymbol{\varepsilon}^L(\mathbf{v}_2)^T \mathbf{C} \boldsymbol{\varepsilon}^L(\delta\mathbf{u}) - \lambda_1 \mathbf{N}^T \boldsymbol{\varepsilon}^N(\mathbf{v}_2, \delta\mathbf{u}) - \alpha_1 \mathbf{N}^T \boldsymbol{\varepsilon}^N(\mathbf{u}_1, \delta\mathbf{u})]\, dA \\
& \quad + \int_{(A)} [\boldsymbol{\varepsilon}^L(\mathbf{u}_1)^T \mathbf{C} \boldsymbol{\varepsilon}^N(\mathbf{u}_1, \delta\mathbf{u}) + \tfrac{1}{2} \boldsymbol{\varepsilon}^N(\mathbf{u}_1, \mathbf{u}_1)^T \mathbf{C} \boldsymbol{\varepsilon}^L(\delta\mathbf{u})]\, dA \Big\} \\
& + \zeta^3 \Big\{ \int_{(A)} [\boldsymbol{\varepsilon}^L(\mathbf{v}_3)^T \mathbf{C} \boldsymbol{\varepsilon}^L(\delta\mathbf{u}) - \lambda_1 \mathbf{N}^T \boldsymbol{\varepsilon}^N(\mathbf{v}_3, \delta\mathbf{u}) - \alpha_1 \mathbf{N}^T \boldsymbol{\varepsilon}^N(\mathbf{v}_2, \delta\mathbf{u}) - \alpha_2 \mathbf{N}^T \boldsymbol{\varepsilon}^N(\mathbf{u}_1, \delta\mathbf{u})]\, dA \\
& \quad + \int_{(A)} [\boldsymbol{\varepsilon}^L(\mathbf{v}_2)^T \mathbf{C} \boldsymbol{\varepsilon}^N(\mathbf{u}_1, \delta\mathbf{u}) + \boldsymbol{\varepsilon}^L(\mathbf{u}_1)^T \mathbf{C} \boldsymbol{\varepsilon}^N(\mathbf{v}_2, \delta\mathbf{u}) + \boldsymbol{\varepsilon}^N(\mathbf{v}_2, \mathbf{u}_1)^T \mathbf{C} \boldsymbol{\varepsilon}^L(\delta\mathbf{u})]\, dA \\
& \quad + \tfrac{1}{2} \int_{(A)} \boldsymbol{\varepsilon}^N(\mathbf{u}_1, \mathbf{u}_1)^T \mathbf{C} \boldsymbol{\varepsilon}^N(\mathbf{u}_1, \delta\mathbf{u})\, dA \Big\} \\
& + \zeta^4 \{ \ldots \} + \ldots
\end{aligned} \tag{2.20}$$

The factor of ζ vanishes due to the buckling condition (2.14). Next the factor of ζ^2 will be equated to zero. The special variation

$$\delta\mathbf{u} = \mathbf{u}_1$$

yields an equation for determining the load coefficient α_1 :

$$\alpha_1 \int \mathbf{N}^T \boldsymbol{\varepsilon}^N(\mathbf{u}_1,\mathbf{u}_1)\, dA = \frac{3}{2} \int \boldsymbol{\varepsilon}^L(\mathbf{u}_1)\, \mathbf{C}\, \boldsymbol{\varepsilon}^N(\mathbf{u}_1,\mathbf{u}_1)\, dA$$

(2.21)

$$\boxed{\alpha_1 = \frac{\lambda_1}{F} \cdot \frac{3}{2} \int \boldsymbol{\varepsilon}^L(\mathbf{u}_1)\, \mathbf{C}\, \boldsymbol{\varepsilon}^N(\mathbf{u}_1,\mathbf{u}_1)\, dA}$$

With the variation

$$\delta \mathbf{u} = \delta \mathbf{v} \ ,$$

where $\delta \mathbf{v}$ is orthogonal to $\mathbf{u}_1$, we get a variational equation for determining $\mathbf{v}_2$:

$$\int_{(A)} [\boldsymbol{\varepsilon}^L(\mathbf{v}_2)^T \mathbf{C}\, \boldsymbol{\varepsilon}^L(\delta \mathbf{v}) - \lambda_1 \mathbf{N}^T \boldsymbol{\varepsilon}^N(\mathbf{v}_2, \delta \mathbf{v})]\, dA$$

(2.22)

$$+ \int_{(A)} [\boldsymbol{\varepsilon}^L(\mathbf{u}_1)^T \mathbf{C}\, \boldsymbol{\varepsilon}^N(\mathbf{u}_1, \delta \mathbf{v}) + \frac{1}{2} \boldsymbol{\varepsilon}^N(\mathbf{u}_1, \mathbf{u}_1)^T \mathbf{C}\, \boldsymbol{\varepsilon}^L(\delta \mathbf{v})]\, dA = 0$$

This will lead to a linear differential equation for $\mathbf{v}_2$, the inhomogeneous part of which depends on the known eigenmode $\mathbf{u}_1$.

The factor of ζ^3 evaluated for the special variation

$$\delta \mathbf{v} = \mathbf{u}_1$$

will yield, with known $\mathbf{u}_1$ and $\mathbf{v}_2$, an equation for the load coefficient α_2:

$$\alpha_2 \int_{(A)} \mathbf{N}^T \boldsymbol{\varepsilon}^N(\mathbf{u}_1,\mathbf{u}_1)\, dA = \int_{(A)} [\boldsymbol{\varepsilon}^L(\mathbf{v}_2)^T \mathbf{C}\, \boldsymbol{\varepsilon}^N(\mathbf{u}_1,\mathbf{u}_1) + 2\boldsymbol{\varepsilon}^L(\mathbf{u}_1)^T \mathbf{C}\, \boldsymbol{\varepsilon}^N(\mathbf{u}_1,\mathbf{v}_2) + \frac{1}{2} \boldsymbol{\varepsilon}^N(\mathbf{u}_1,\mathbf{u}_1)^T \mathbf{C}\, \boldsymbol{\varepsilon}^N(\mathbf{u}_1,\mathbf{u}_1)]\, dA$$

(2.23)

$$\alpha_2 = \frac{\lambda_1}{F} \int_{(A)} [\boldsymbol{\varepsilon}^L(\mathbf{v}_2)^T \mathbf{C}\, \boldsymbol{\varepsilon}^N(\mathbf{u}_1,\mathbf{u}_1) + 2\boldsymbol{\varepsilon}^L(\mathbf{u}_1)^T \mathbf{C}\, \boldsymbol{\varepsilon}^N(\mathbf{u}_1,\mathbf{v}_2) + \frac{1}{2} \boldsymbol{\varepsilon}^N(\mathbf{u}_1,\mathbf{u}_1)^T \mathbf{C}\, \boldsymbol{\varepsilon}^N(\mathbf{u}_1,\mathbf{u}_1)]\, dA$$

By evaluating factors of powers higher than ζ^3 the solution can theoretically be traced further into the advanced postbuckling region. This approach will not be followed here. At the present time we confine our interest to the initial postbuckling behaviour.

2.2.4 Load-"shortening" relation

The potential energy of thin shells, equ. (2.12), can be written as

$$\Pi = W - \lambda V \tag{2.24}$$

where W is the potential energy of the internal forces or elastic energy, while λV is the potential energy of external loads. The quantity V may be considered as a generalized shortening.

The prebuckling displacements depend linearly on the load factor λ,

$$\hat{\mathbf{u}} = \lambda \mathbf{u}_0 \quad . \tag{2.25}$$

Instead of (2.9) we may write, therefore,

$$\hat{\Pi} = \lambda^2 \left(\frac{1}{2} \int_{(A)} \boldsymbol{\varepsilon}^L(\mathbf{u}_0)^T \mathbf{C}\, \boldsymbol{\varepsilon}^L(\mathbf{u}_0)\, dA - \int_{(S_N)} \hat{\mathbf{N}}^T \mathbf{u}_0\, dS \right)$$

We substitute this in the potential energy (2.12) and get, in view of equ. (2.29),

$$W = \frac{1}{2} \int_{(A)} \left[\boldsymbol{\varepsilon}^L(\mathbf{u}^*)^T \mathbf{C} \boldsymbol{\varepsilon}^L(\mathbf{u}^*) + \boldsymbol{\varepsilon}^L(\mathbf{u}^*)^T \mathbf{C} \boldsymbol{\varepsilon}^N(\mathbf{u}^*,\mathbf{u}^*) + \frac{1}{4} \boldsymbol{\varepsilon}^N(\mathbf{u}^*,\mathbf{u}^*)^T \mathbf{C} \boldsymbol{\varepsilon}^N(\mathbf{u}^*,\mathbf{u}^*) \right] dA$$

$$V = \lambda \left[-\frac{1}{2} \int_{(A)} \boldsymbol{\varepsilon}^L(\mathbf{u}_0)^T \mathbf{C}\, \boldsymbol{\varepsilon}^L(\mathbf{u}_0)\, dA + \int_{(S_N)} \tilde{\mathbf{N}}^T \boldsymbol{\varepsilon}^N(\mathbf{u}_0)\, dS \right] + \frac{1}{2} \int_{(A)} \mathbf{N}^T \boldsymbol{\varepsilon}^N(\mathbf{u}^*,\mathbf{u}^*)\, dA \quad . \tag{2.26}$$

In the prebuckling range the displacement $\mathbf{u}^*$ is zero. The generalized shortening is

$$V = V_0 = \lambda \Pi_0 \quad ,$$

the prebuckling compliance being

$$\frac{1}{K_0} = \frac{dV_0}{d\lambda} = \Pi_0$$

or

$$\frac{1}{K_0} = -\frac{1}{2} \int_{(A)} \boldsymbol{\varepsilon}^L(\mathbf{u}_0)\, \mathbf{C}\, \boldsymbol{\varepsilon}^L(\mathbf{u}_0)\, dA + \int_{(S_N)} \tilde{\mathbf{N}}_0^T(\mathbf{u}_0)\, dS \quad .$$

In a linear system the value of the second integral is twice that of the first one, since it is twice the work performed by the edge loads $\tilde{\mathbf{N}}_0$ when increasing from zero to the given magnitude. This, in turn, is the work stored in the shell as elastic energy. Thus we get

$$\frac{1}{K_0} = \frac{1}{2}\int_{(A)} \boldsymbol{\varepsilon}^L(\mathbf{u}_0)^T \mathbf{C}\, \boldsymbol{\varepsilon}^L(\mathbf{u}_0)\, dA \quad . \tag{2.27}$$

For computation the alternative form

$$\frac{1}{K_0} = \frac{1}{2}\int_{(A)} \mathbf{N}_0^T\, \mathbf{C}^{-1}\, \tilde{\mathbf{N}}_0\, dA \tag{2.28}$$

may sometimes be useful.

The generalized displacement along the bifurcating path is

$$V - V_0 = \frac{1}{2}\int_{(A)} \mathbf{N}^T \boldsymbol{\varepsilon}^N(\mathbf{u}^*,\mathbf{u}^*)\, dA \quad .$$

Substituting the expansion (2.18) yields

$$\begin{aligned} V - V_0 &= \frac{1}{2}\int_{(A)} \mathbf{N}^T \boldsymbol{\varepsilon}^N(\zeta\mathbf{u}_1 + \zeta^2\mathbf{v}_2 + \cdots\,,\, \zeta\mathbf{u}_1 + \zeta^2\mathbf{v}_2 + \cdots)\, dA \\ &= \frac{1}{2}\zeta^2\Big[\int_{(A)} \mathbf{N}^T \boldsymbol{\varepsilon}^N(\mathbf{u}_1,\mathbf{u}_1) + \zeta^2\int_{(A)} \mathbf{N}^T \boldsymbol{\varepsilon}^N(\mathbf{v}_2,\mathbf{v}_2) + \cdots\Big] \\ &= \frac{1}{2}\zeta^2 F\left[\frac{1}{\lambda_1} + \frac{\zeta^2}{\lambda_2} + \cdots\right] , \\ V - V_0 &\approx \frac{1}{2}\zeta^2\,\frac{F}{\lambda_1} \end{aligned}$$

Solving for ζ^2 yields

$$\zeta^2 = \frac{2\lambda_1}{F}(V - V_0) \quad , \tag{2.29}$$

hence

$$\lambda = \lambda_1 + \alpha_1 \zeta + \alpha_2 \zeta^2 + \cdots$$

(2.30)

$$= \lambda_1 + \alpha_1 \sqrt{\frac{2\lambda_1}{F}(V - V_0)} + \alpha_2 \frac{2\lambda_1}{F}(V - V_0) + \cdots$$

This formula shows λ as a function of V and V_o, and we conclude

$$d\lambda = \frac{\partial \lambda}{\partial V} dV + \frac{\partial \lambda}{\partial V_0} dV_0 = \frac{\partial \lambda}{\partial V} dV + \frac{\partial \lambda}{\partial V_0} \frac{dV_0}{d\lambda} d\lambda$$

(2.31)

$$K = \frac{d\lambda}{dV} = \frac{\partial \lambda}{\partial V} \Big/ \left(1 - \frac{\partial \lambda}{\partial V_0} \frac{1}{K_0}\right)$$

$$\frac{K}{K_0} = \frac{\partial \lambda}{\partial V} \Big/ \left(K_0 - \frac{\partial \lambda}{\partial V_0}\right)$$

In the vicinity of the bifurcation point the difference $V-V_o$ may be considered as small as desired. Thus we get from equs. (2.30) and (2.31)

1) for $\alpha_1 \neq 0$

$$\frac{K}{K_0} = \lim_{V - V_0 \to 0} \left(- \alpha_1 \frac{2 \frac{\lambda_1}{F}}{2\sqrt{\frac{2\lambda_1}{F}(V - V_0)} \left(K_0 + \frac{\alpha_1 \cdot 2 \frac{\lambda_1}{F}}{2\sqrt{\frac{2\lambda_1}{F}(V - V_0)}} \right)} \right) = 1 \quad ,$$

meaning that the bifurcating path in the load-shortening diagram initially goes back along the fundamental path, and,

2) for $\alpha_1 = 0$

(2.32)

$$\boxed{\frac{K}{K_0} = \alpha_2 \frac{2 \frac{\lambda_1}{F}}{K_0 + \alpha_2 \frac{2\lambda_1}{F}} = \frac{1}{1 + K_0 \frac{F}{2\alpha_2 \lambda_1}}}$$

3. Numerical Evaluation of Analytical Relations

3.1 Modal Analysis

The numerical procedure to be applied for the evaluation of the

formulae derived in the preceding chapter is based on the computer program BEOS (Buckling of Eccentrically Orthotropic Sandwich Shells) which is capable of computing a prescribed number of eigenmodes $\mathbf{u}_i$ and eigenvalues λ_i.

Knowing several eigenmodes it is reasonable to expand the displacements $\mathbf{v}_2$ into a series of these modes. However, due to (2.19) $\mathbf{u}_1$ must not be contained in this expansion. Thus

$$\mathbf{v}_2 = \sum_{k=2}^{h} a_2^k \mathbf{u}_k \,. \tag{3.1}$$

Substituting this series into the variational equation (2.22) from which $\mathbf{v}_2$ is to be determined we get

$$\sum_{k=2}^{h} \left\{ a_2^k \int_{(A)} [\boldsymbol{\varepsilon}^L(\mathbf{u}_k)^T \mathbf{C}\, \boldsymbol{\varepsilon}^L(\delta\mathbf{v}) - \lambda_1 \mathbf{N}^T \boldsymbol{\varepsilon}^N(\mathbf{u}_k, \delta\mathbf{v})]\, dA \right\}$$

$$= - \int_{(A)} [\boldsymbol{\varepsilon}^L(\mathbf{u}_1)^T \mathbf{C}\, \boldsymbol{\varepsilon}^N(\mathbf{u}_1, \delta\mathbf{v}) + \frac{1}{2} \boldsymbol{\varepsilon}^N(\mathbf{u}_1, \mathbf{u}_1)^T \mathbf{C}\, \boldsymbol{\varepsilon}^L(\delta\mathbf{v})]\, dA$$

With $\delta\mathbf{v} = \mathbf{u}_2, \mathbf{u}_3, \ldots$ making use of the orthonormalization (2.17) and (2.19) we get equations for the coefficients $a_2{}^k$:

$$a_2^k = \frac{-\lambda_k}{F(\lambda_k - \lambda_1)} \int_{(A)} [\boldsymbol{\varepsilon}^L(\mathbf{u}_1)^T \mathbf{C}\, \boldsymbol{\varepsilon}^N(\mathbf{u}_1, \mathbf{u}_k) + \frac{1}{2} \boldsymbol{\varepsilon}^L(\mathbf{u}_k)^T \mathbf{C}\, \boldsymbol{\varepsilon}^N(\mathbf{u}_1, \mathbf{u}_1)]\, dA. \tag{3.2}$$

From (2.23) and (2.24) we get

$$\alpha_2 = \frac{\lambda_1}{F} \left\{ \sum_{k=2}^{h} 2a_2^k \int_{(A)} [\boldsymbol{\varepsilon}^L(\mathbf{u}_1)^T \mathbf{C}\, \boldsymbol{\varepsilon}^N(\mathbf{u}_1, \mathbf{u}_k) + \frac{1}{2} \boldsymbol{\varepsilon}^L(\mathbf{u}_k)^T \mathbf{C}\, \boldsymbol{\varepsilon}^N(\mathbf{u}_1, \mathbf{u}_1)]\, dA \right.$$

$$\left. + \frac{1}{2} \int_{(A)} \boldsymbol{\varepsilon}^N(\mathbf{u}_1, \mathbf{u}_1)\, \mathbf{C}\, \boldsymbol{\varepsilon}^N(\mathbf{u}_1, \mathbf{u}_1)\, dA \right\} .$$

Regarding (3.2) this may be transformed to

$$(3.3)\qquad \boxed{\alpha_2 = 2\lambda_1 \left[\frac{1}{4F} \int_{(A)} \boldsymbol{\varepsilon}^N(\mathbf{u}_1,\mathbf{u}_1)^T \mathbf{C}\, \boldsymbol{\varepsilon}^N(\mathbf{u}_1,\mathbf{u}_1)\, dA - \sum_{k=2}^{h} \frac{\lambda_k - \lambda_1}{\lambda_k} (a_2^k)^2 \right]} \quad .$$

3.2 Evaluation of Integrals

The load coefficients α_1, α_2 and the expansion coefficients, as presented in equs. (2.21), (3.3) and (3.2) are numerically determined by evaluating the integrals

$$(3.4)\qquad \begin{aligned} I31 &= \int_{(A)} \boldsymbol{\varepsilon}^L(\mathbf{u}_k)^T \mathbf{C}\, \boldsymbol{\varepsilon}^N(\mathbf{u}_1,\mathbf{u}_1)\, dA \\ I33 &= \int_{(A)} \boldsymbol{\varepsilon}^L(\mathbf{u}_1)^T \mathbf{C}\, \boldsymbol{\varepsilon}^N(\mathbf{u}_1,\mathbf{u}_k)\, dA \\ I4 &= \int_{(A)} \boldsymbol{\varepsilon}^N(\mathbf{u}_1,\mathbf{u}_1)^T \mathbf{C}\, \boldsymbol{\varepsilon}^N(\mathbf{u}_1,\mathbf{u}_1)\, dA \end{aligned}$$

The integrands are sums of expressions like

$$C_{12} \cdot \frac{\partial u_k}{\partial x} \frac{\partial w_1}{\partial y} \frac{\partial w_1}{\partial y} = C_{12} \frac{\partial u_k^2}{\partial x} \frac{\partial u_1^1}{\partial y} \frac{\partial u_1^1}{\partial y}$$

(for definition of $\mathbf{u}_k^n$ see equ. (2.1)), or

$$2C_{13} \cdot \frac{\partial w_1}{\partial x} \frac{\partial w_1}{\partial x} \frac{\partial w_1}{\partial x} \frac{\partial w_1}{\partial y} = 2C_{13} \frac{\partial u_1^1}{\partial x} \frac{\partial u_1^1}{\partial x} \frac{\partial u_1^1}{\partial x} \frac{\partial u_1^1}{\partial y} \quad .$$

Generally speaking, the terms of the integrands have the form

$$(3.5)\qquad T = c \cdot \prod_{\alpha=1}^{\beta} \frac{\partial^{\nu_\alpha + \mu_\alpha} u^{i_\alpha}_{m_\alpha}}{\partial x^{\nu_\alpha}\, \partial y^{\mu_\alpha}}$$

with $\beta = 3$ or $\beta = 4$, resp.; ν_α , $\mu_\alpha = 0/1/2$; $i_\alpha = 1/2/3/4/5$ and $m_\alpha = 1,2 \ldots n$.

Each term is identified by the 4β numbers $\nu_\alpha, \mu_\alpha, i_\alpha, n_\alpha = 1,2 \ldots \beta$, and by the numerical factor c. A list of terms can be established according to the definition of the strain vectors $\boldsymbol{\varepsilon}^L(\mathbf{u})$ and $\boldsymbol{\varepsilon}^N(\mathbf{u}_j, \mathbf{u}_k)$ equ. (2.4). We shall now outline the method used to compute the contribution of one typical term to the integrals, equ. (3.4).

In the computer program BEOS the shell is divided, by straight lines running parallel to the edges, into rectangular subregions. Within each subregion the displacement components $u^1, u^2 \ldots = w, u, \ldots$ are approximated by interpolation based on certain values known at the corners of the subregion, see ref. [7]. These basic data, e.g. for the displacement w, are

$$w \ , \ \frac{\partial w}{\partial x} \ , \ \frac{\partial w}{\partial y} \ , \ \frac{\partial^2 w}{\partial x \partial y}$$

meaning that for each component of the displacement vector 16 values have to be known for a subregion to perform the interpolation. As the displacement vector has 5 components for a sandwich shell (cf. equ. (2.1)), a total of 80 values have to be known to completely describe the deformation within each subregion. Thinking in terms of the finite element method this would mean that we work with a conforming element having 80 elemental degrees of freedom.

Let the subregion (or finite element) under consideration be the j-th one in the x-direction and the k-th one in the y-direction. The side lengths are a_j and b_k respectively. We define a local coordinate system (ξ, η) with $0 \leq \xi, \eta \leq 1$, from which the local coordinates x,y are obtained due to

$$x = x_j + a_j \xi \ ,$$

$$y = y_k + b_k \eta \ . \qquad (3.6)$$

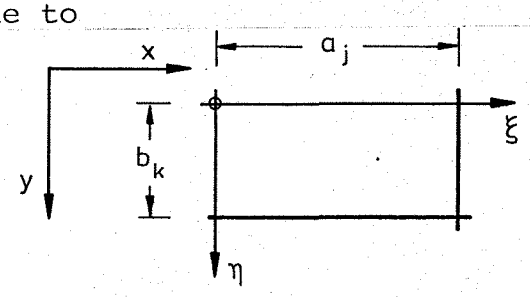

From the values and derivatives of the i-th displacement function in the n-th eigenmode we form a matrix

(3.7)

$\overset{i}{\breve{U}}_{n,pq} =$

p \ q	1	2	3	4
1	$u_n^i\,(0,0)$	$\frac{\partial u_n^i}{\partial \eta}(0,0)$	$u_n^i\,(0,1)$	$\frac{\partial u_n^i}{\partial \eta}(0,1)$
2	$\frac{\partial u_n^i}{\partial \xi}(0,0)$	$\frac{\partial^2 u_n^i}{\partial \xi\,\partial \eta}(0,0)$	$\frac{\partial u_n^i}{\partial \xi}(0,1)$	$\frac{\partial^2 u_n^i}{\partial \xi\,\partial \eta}(0,1)$
3	$u_n^i\,(1,0)$	$\frac{\partial u_n^i}{\partial \eta}(1,0)$	$u_n^i\,(1,1)$	$\frac{\partial u_n^i}{\partial \eta}(1,1)$
4	$\frac{\partial u_n^i}{\partial \xi}(1,0)$	$\frac{\partial^2 u_n^i}{\partial \xi\,\partial \eta}(1,0)$	$\frac{\partial u_n^i}{\partial \xi}(1,1)$	$\frac{\partial^2 u_n^i}{\partial \xi\,\partial \eta}(1,1)$

Within the subregion the values of the function $u_n^i(\xi,\eta)$ are, by interpolation

$$u_n^i(\xi,\eta) = \sum_{p=1}^{4}\sum_{q=1}^{4} \overset{i}{\breve{U}}_{n,pq}\,\phi_p(\eta)\,\phi_q(\xi)\,.$$

In this formula the functions $\phi_p(\eta)$, $\phi_q(\xi)$ are the four cubic Hermite polynomials

The derivatives of $u_n^i(\xi,\eta)$ are

(3.8) $$\frac{\partial^{\nu+\mu} u_n^i}{\partial x^\nu\,\partial y^\mu}(\xi,\eta) = \frac{1}{a_j^\nu\, b_k^\mu}\sum_{p=1}^{4}\sum_{q=1}^{4} \overset{i}{\breve{U}}_{n,pq}\,\psi_p^\mu(\eta)\,\psi_q^\nu(\xi)$$

with

(3.9) $$\psi_r^\varrho(\zeta) = \frac{d^\varrho \phi_r}{d\zeta^\varrho}(\zeta)\,.$$

Substituing (3.8), (3.9) into (3.5) yields, for the integrands,

$$T = c \cdot \prod_{\alpha=1}^{\beta} \frac{1}{a_j^{\nu_\alpha} b_k^{\mu_\alpha}} \sum_{p_\alpha=1}^{4} \sum_{q_\alpha=1}^{4} \tilde{U}^{i_\alpha}_{m_\alpha, p_\alpha q_\alpha} \psi^{\mu_\alpha}_{p_\alpha}(\eta)\, \psi^{\nu_\alpha}_{q_\alpha}(\xi)$$

which is the same as

$$T = \frac{c}{a^{(\sum_{\alpha=1}^{\beta}\nu_\alpha)}\, b^{(\sum_{\alpha=1}^{\beta}\mu_\alpha)}} \left\{ \sum_{p_1=1}^{4} \left(\sum_{q_1=1}^{4} \left[\sum_{p_2=1}^{4} \left(\sum_{q_2=1}^{4} \left[\ldots \left[\sum_{p_\beta=1}^{4} \left(\sum_{q_\beta=1}^{4} \prod_{\alpha=1}^{\beta} \tilde{U}^{i_\alpha}_{m_\alpha, p_\alpha q_\alpha} \psi^{\mu_\alpha}_{p_\alpha}(\eta) \psi^{\nu_\alpha}_{q_\alpha}(\xi) \right) \right] \ldots \right] \right) \right] \right) \right\} .$$

This sum of functions has to be integrated over the area A_{ij} of the subregion. The integrals to be computed are

$$\int_{(A_{i,j})} \prod_{\alpha=1}^{\beta} \psi^{\mu_\alpha}_{p_\alpha}(\eta)\, \psi^{\nu_\alpha}_{q_\alpha}(\xi)\, dA = a_j\, b_k \int_0^1 \prod_{\alpha=1}^{\beta} \psi^{\mu_\alpha}_{p_\alpha}(\eta)\, d\eta \cdot \int_0^1 \prod_{\alpha=1}^{\beta} \psi^{\nu_\alpha}_{q_\alpha}(\xi)\, d\xi \quad .$$

The functions under the integrals are known. They can be computed and stored once and forever. We write

$$\Theta^{\varrho_\alpha}_{\beta, r_\alpha} = \int_0^1 \prod_{\alpha=1}^{\beta} \psi^{\varrho_\alpha}_{r_\alpha}(\zeta)\, d\zeta \qquad (3.10)$$

and get, for the contribution of a subregion to the integral over one typical term,

$$J_{i,j} = \frac{c}{a^{(\sum_{\alpha=1}^{\beta}\nu_\alpha - 1)}\, b^{(\sum_{\alpha=1}^{\beta}\mu_\alpha - 1)}} \left\{ \sum_{p_1=1}^{4} \left(\sum_{q_1=1}^{4} \left[\sum_{p_2=1}^{4} \left(\sum_{q_2=1}^{4} \left[\ldots \left[\sum_{p_\beta=1}^{4} \left(\sum_{q_\beta=1}^{4} \prod_{\alpha=1}^{\beta} \tilde{U}^{i_\alpha}_{m_\alpha, p_\alpha q_\alpha} \Theta^{\mu_\alpha}_{\beta p_\alpha} \Theta^{\nu_\alpha}_{\beta q_\alpha} \right) \right] \ldots \right] \right) \right] \right) \right\} \qquad (3.11)$$

To determine the integrals (3.4) these contributions have to be computed and summed up for all terms of the integrands and for all subregions.

One item remains to be mentioned: Most of the components in the matrix

$$\tilde{U}^{i}_{n,pq} \quad , \qquad \text{equ. (3.6)}$$

are derivatives of the displacement $u_n^i(x,y)$. They are taken with respect to the local coordinates (ξ,η). However, the derivatives computed and stored by the program BEOS are taken with respect to a global normalized coordinate system

$$\tilde{x} = \frac{\pi}{l_x} x \quad ; \quad \tilde{y} = \frac{\pi}{l_y} y$$

where l_x and l_y are the panel dimensions in the x- and y-direction:

$$l_x = \sum_{(j)} a_j \quad ; \quad l_y = \sum_{(k)} b_k \quad .$$

For the transformation of this system to the local system (ξ,η) we find from equ. (3.6)

$$\tilde{x} = \tilde{x}_j + \frac{\pi a_j}{l_x} \xi \quad ; \quad \tilde{y} = \tilde{y}_k + \frac{\pi b_k}{l_y} \eta \quad ,$$

and it follows that

$$\frac{\partial}{\partial \xi} = \frac{\pi a_j}{l_x} \frac{\partial}{\partial \tilde{x}} \quad , \quad \frac{\partial}{\partial \eta} = \frac{\pi b_k}{l_y} \frac{\partial}{\partial \tilde{y}} \quad . \tag{3.12}$$

This transformation has to be taken into account in establishing the matrices defined in equ. (3.7)

3.3 Choice of Normalizing Factor F

The parameters α_1, α_2, as they follows from equs. (2.21) and (3.3), depend on the normalizing factor F. By different choices of F they may be made big or small. Some guide is needed for chosing F properly.

It seems to be reasonable to link ζ, or ζ^2, more directly to (V-Vo). We normalize (V-Vo) in equ. (2.30), dividing it by

(3.13) $$V_1 = \lambda_1 / K_0$$

and get

$$\frac{\lambda}{\lambda_1} = 1 + \alpha_1 \sqrt{\frac{2}{FK_0} \frac{V-V_0}{V_1}} + \alpha_2 \frac{2\lambda_1}{FK_0} \frac{V-V_0}{V_1} .$$

If we take

(3.14) $$\zeta = \sqrt{\frac{V-V_0}{V_1}} , \quad \bar{\alpha}_1 = \alpha_1 \sqrt{\frac{2}{FK_0}} , \quad \bar{\alpha}_2 = \alpha_2 \frac{2\lambda_1}{FK_0}$$

we can write

(3.15) $$\frac{\lambda}{\lambda_1} = 1 + \bar{\alpha}_1 \zeta + \bar{\alpha}_2 \zeta^2 .$$

This choice corresponds to taking

$$F = 2/Ko .$$

3.4 Influence of Symmetry or Anti-Symmetry of Buckling Modes on the Integrals over Triple on Quadruple Products

Very frequently the buckling modes are symmetric or anti-symmetric with respect to the center lines of the panels. We may consider the center lines as coordinate axes (x,y). Then a mode is called symmetric in the x-direction (i.e. with respect to the y-axis) if its normal displacement is

$$w(-x,y) = w(x,y) ,$$

and anti-symmetric in the x-direction if

$$w(-x,y) = w(x,y)$$

A corresponding definition holds for symmetry or anti-symmetry in the y-direction (i.e. with respect to the x-axis).

We consider four cases of symmetry properties as presented in the following table:

case no.	1	2	3	4
x - direction, y-direction	s, s	a, s	s, a	a, a

s: symmetric a: anti-symmetric

The symmetry properties of the three non-vanishing components of the vector

$$\boldsymbol{\varepsilon}^N(\mathbf{u}_1, \mathbf{u}_2) = \boldsymbol{\varepsilon}^N(\mathbf{u}_2, \mathbf{u}_1) \quad ,$$

for all possible combinations, are compiled in the next table,

property of $\mathbf{u}_1/\mathbf{u}_2$	s,s/s,s	s,s/a,s	s,s/s,a	s,s/a,a	a,s/a,s	a,s/s,a	a,s/a,a	s,a/s,a	s,a/a,a	a,a/a,a
" " $\varepsilon_1^N(\mathbf{u}_1,\mathbf{u}_2)$	s, s	a, s	s, a	a, a	s, s	a, a	s, a	s, s	a, s	s, s
" " $\varepsilon_2^N(\mathbf{u}_1,\mathbf{u}_2)$	s, s	a, s	s, a	a, a	s, s	a, a	s, a	s, s	a, s	s, s
" " $\varepsilon_3^N(\mathbf{u}_1,\mathbf{u}_2)$	a, a	s, a	a, s	s, s	a, a	s, s	a, s	a, a	s, a	a, a

and the symmetry properties of $\mathbf{C}\,\boldsymbol{\varepsilon}^L(\mathbf{u}_i) = \mathbf{N}_i$ are as follows:

property of $\mathbf{u}_i$	s, s	a, s	s, a	a, a
" " $N_{i,1}$	s, s	a, s	s, a	a, a
" " $N_{i,2}$	s, s	a, s	s, a	a, a
" " $N_{i,3}$	a, a	s, a	a, s	s, s

The integrands of the integrals over triple products are inner products of $\mathbf{N}_i$ and $\boldsymbol{\varepsilon}^N(\mathbf{u}_j, \mathbf{u}_i)$.

$$I_{ijk} = \mathbf{N}_i^T \boldsymbol{\varepsilon}^N(\mathbf{u}_j, \mathbf{u}_k) = \boldsymbol{\varepsilon}^L(\mathbf{u}_i)^T \mathbf{C}\, \boldsymbol{\varepsilon}^N(\mathbf{u}_j, \mathbf{u}_k) \quad .$$

Only doubly symmetric parts will contribute to the integrals.

The symmetry properties of the three modes involved may be characterized by the triplets

[property of $\mathbf{u}_i$ / property of $\mathbf{u}_j$ / property of $\mathbf{u}_k$]

We find that only the following combinations give rise to doubly symmetric integrands:

[s,s/s,s/s,s] , [s,s/a,s/a,s] , [s,s/s,a/s,a] , [s,s/a,a/a,a] ,

[a,s/s,s/a,s] , [a,s/s,a/a,a] ,

[s,a/s,s/s,a] , [s,a/a,s/a,a] ,

[a,a/s,s/a,a] , [a,a/a,s/s,a] .

It is obvious that these triplets must be symmetric with respect to the second and third entry, i.e. if [p_1 / p_2 / p_3] leads to a doubly symmetric integrand then does also [p_1 / p_3 / p_2]. Moreover the list above shows that a corresponding symmetry property holds for the first and second entry. Therefore the list may be reduced to

[s,s/s,s/s,s] , [s,s/a,s/a,s] , [s,s/s,a/s,a] , [s,s/a,a/a,a] , [a,s/s,a/a,a]

with the additional statement that a doubly symmetric integrand will result for any order of the three entries.

Analysis of the initial postbuckling behaviour requires evaluation of only such integrals over triple products where two of the modes involved are equal to the buckling mode. Of all triplets only those having at least two equal entries need be retained, viz.

[s,s/s,s/s,s] , [s,s/a,s/a,s] , [s,s/s,a/s,a] , [s,s/a,a/a,a] .

In each of these triplets there is at least one entry s,s. Thus any buckling mode will combine to non-zero integrals over triple products, with doubly symmetric higher modes only.

Similar considerations for the quadruple product integrands

$$I_{ijkl} = \boldsymbol{\varepsilon}^N(\mathbf{u}_i, \mathbf{u}_j)^T \mathbf{C}\, \boldsymbol{\varepsilon}^N(\mathbf{u}_k, \mathbf{u}_l)$$

lead to the combinations

$$[s,s/s,s/s,s/s,s],[s,s/s,s/a,s/a,s],[s,s/s,s/s,a/s,a],$$
$$[s,s/s,s/a,a/a,a],[s,s/a,s/s,a/a,a],[a,s/a,s/a,s/a,s],$$
$$[a,s/a,s/s,a/s,a],[a,s/a,s/a,a/a,a],[s,a/s,a/s,a/s,a],$$
$$[s,a/s,a/a,a/a,a],[a,a/a,a/a,a/a,a].$$

Again a doubly symmetric integrand will result for any permutation of the four entries.

4. Examples

4.1 Influence of In-Plane Boundary Conditions on the Initial Postbuckling Behaviour of Isotropic Curved Panels

As a first example the buckling behaviour of two isotropic curved panels with hinged edges will be considered.

This problem was already studied by W.T. KOITER [5]. However, for the present examples the in-plane boundary conditions were chosen different from those considered in KOITER's study. The panels were supposed to be loaded by controlled shortening leading to boundary conditions $u^* = 0$. The deflections v^* were likewise assumed to be zero all along the edges. Both panels were given equal width and length, but the radii of curvature were different.

A complete information on the geometry of the panels is presented in Fig. 2, whereas the buckling loads and the initial postbuckling paths are shown on Fig. 3. It should be mentioned that the buckling modes of the two panels exhibit two half waves in the direction of the load, and one half wave in the transverse direction. Thus they are anti-symmetrical/symmetrical (a,s).

Panel No. 1 has a positive, although very low, postbuckling stiffness. Panel No. 2, i.e. the more curved one, has a higher buckling load but a negative postbuckling stiffness. The shell with zero slope of the load-shortening curve in the postbuckling range would be somewhere between te two. Its curvature parameter

$$\Theta = \sqrt[4]{\frac{12\,(1-\nu^2)}{2}}\;\frac{b}{\sqrt{r\,t}} \tag{4.1}$$

would be in the range

$$1.195 < \Theta < 1.311 .$$

KOITER found for the weaker "classical" boundary conditions treated by him, the postbuckling curve with zero slope at panels with

$$\Theta = 0.64.$$

He supposed that the boundary conditions would influence this value strongly. The present result confirms his supposition.

It might be interesting to know that, for the second panel, out of the higher buckling modes the 2nd (3.1)*) and the 9th (1.1) one are doubly symmetric. They influence the computational value for the postbuckling stiffness. The deformation pattern in the initial postbuckling range is

$$u^* = \zeta\, u_1 + \zeta^2\,(\,0{,}0514\, u_2 + 0{,}0225\, u_q\,)$$

*) Occasionally buckling modes will be roughly characterized by pairs of integer numbers (m,n), giving the numbers of half waves in the x- and y-direction, respectively.

4.2 Initial Postbuckling Behaviour of Short Isotropic Panels

The panels considered in the preceding paragraph were modified in two respects: The radius was reduced to r = 554 mm, and the unloaded edges were clamped. Shells of different lengths were analysed for their buckling loads and modes. Two of them were then selected for being analysed with respect to their initial postbuckling behaviour.

The first panel is 69.36 mm long. It buckles in the symmetrical (1.1)-mode. The second panel is 76.65 mm long. It buckles in the anti-symmetrical (2.1)-mode. The buckling loads of the two panels are nearly equal.

For the first panel the result is quite unusual, though not unexpected. It cannot be compared to any of the published solutions on the postbuckling behaviour of curved panels, since it predicts non-symmetrical bifurcation with $\alpha_1 \neq 0$.

All the published investigations on the initial postbuckling behaviour of panels, as far as the author is aware, found symmetrical bifurcation with $\alpha_1 = 0$ meaning that the postbuckling behaviour is independent of the sign of the postbuckling deflection. In other words: No matter whether the shell buckles inward or outward, the initial postbuckling behaviour is the same. It is surprising that this statement should hold not only for plane panels for which an inward or outward direction cannot be defined, but also for curved panels. If the buckling mode is anti-symmetrical, however, than for each part buckling inward there is a counterpart buckling outward. It is obvious that in this case the bifurcation is symmetrical. It is this case which was treated throughout in past studies.

Figs. 4 and 5 show the initial postbuckling behaviour of the two panels. The curves for the longer panel deserve no discussion as they depict the familiar symmetrical bifurcation with a slightly negative postbuckling stiffness. The shorter panel exhibits an unsymmetrical bifurcation behaviour. If we would regard strictly the asymptotic nature of the theory we should stop the computa-

tion as soon as a non-zero value for α_1 is found. This would yield a straight line in Fig. 4, and we would conclude that the panel is not capable of carrying additional loads after buckling. We would arrive at such a conclusion for any short curved panel whatever small its curvature might be. On the other hand for a slightly longer shallow panel the buckling mode of which is anti-symmetrical we might get $\alpha_1 = 0$ and $\alpha_2 > 0$ meaning that this panel would well be able to carry loads higher than the buckling load.

A result of this kind is quite unreasonable. It was hoped that by taking the coefficient α_2, in addition to α_1, into consideration more consistancy would be achieved. But now the two values of α_2 are very dissimilar indicating totally different postbuckling behaviour for two panels of only slightly different dimensions.

Probably the contradiction can be resolved by improved techniques for taking into account the coupling of neighbouring modes, i.e. of modes connected with nearly equal buckling loads. This must be left to a later study.

4.3 Test Panels under Idealized Loads

4.3.1 Dimensions and Elastic Properties of the Panels

A series of tests was performed on orthotropic sandwich panels. A first report was presented earlier [1]. The test specimens had a quadratic plan view with dimensions 800 x 800 mm². They were cylindrically curved with the straight generators in the direction of the main compressive load. Three-layer sandwich construction was chosen (see Fig 6). The core consisted of PVC foam with a density ranging from 30 kg/m³ to 50 kg/m³. The face layers were built-up of three thin plies of glass fabric reinforced epoxy. For the inner and outer ply of each face layer a nearly unidirectional fabric was used, with 93% of the fibres oriented parallel to the generators, whereas for the intermediate plies bidirectional twill fabric was oriented at 45 degrees.

Most of the elastic properties of the panels were determined in an extensive test program. The extensional stiffnesses B_{ij} were found to be

$$B_{11} = 39\ 700 \text{ N/mm}, \qquad B_{12} = 8\ 580 \text{ N/mm},$$
$$B_{22} = 20\ 500 \text{ N/mm}, \qquad B_{33} = 8\ 350 \text{ N/mm}.$$

The panels No. 1 and No. 2 had core heights of h = 8 mm. The tests with these panels will not be evaluated in this report.

The nominal core heights of panels No. 3, 4 and 5 were only 6 mm. Their bending stiffnesses were

$$K_{11} = 458\ 000 \text{ N/mm}, \qquad K_{12} = 98\ 900 \text{ N/mm},$$
$$K_{22} = 236\ 000 \text{ N/mm}, \qquad K_{33} = 96\ 200 \text{ N/mm}.$$

The extensional and bending stiffnesses have to be supplemented by more stiffness properties in order to describe the properties of the panels completely [7]. However, for the purpose of this report the given properties should suffice.

The test panels No. 4 and 5 were nominally equal, whereas panel No. 3 had a different radius of curvature. The radii were

Panel No. 3: r = 3213 mm (shell rise h = 25 mm)
Panels No. 4, 5: r = 1625 mm (shell rise h = 50 mm)

4.3.2 Results of Computations

For each of the two configurations buckling modes and the corresponding bifurcation loads were computed, followed by a calculation of the parameters $\bar{\alpha}_1$ and $\bar{\alpha}_2$ characterizing the initial postbuckling behaviour. Two load systems were assumed:

1) Constant axial compression,
2) Simultaneous axial compression and shear with $N_{xo} = 100$ N/mm, $N_{xyo} = 10$ N/mm.

the bifurcation loads were computed as factors by which these loads have to be multiplied.

In Table 1 the results of the computations are compiled. The three lowest eigenvalues λ are presented in order to judge whether mode coupling renders the analysis unvalid. The symmetry properties of the buckling modes can be defined for the case of pure compression only. The modes under simultaneous compression and shear are similar, but somewhat distorted, Fig. 7. Therefore characterization of their properties is put into parantheses.

Next the parameters $\bar{\alpha}_1$ and $\bar{\alpha}_2$ are presented. They define a parabola in the diagram λ/λ_1 vs. ζ . In the case of symmetrical bifurcation the apex of the parabola is at the point $\zeta = 0$, $\lambda/\lambda_1 = 1$. With unsymmetric bifurcation the parabola if offset.

As an example the buckling modes of panels No. 4 and 5 are shown on Fig. 7 for the two load cases. The values of ζ_{min} and $1-(\lambda/\lambda_1)_{min}$ specifying the amount of this offset are presented, too.

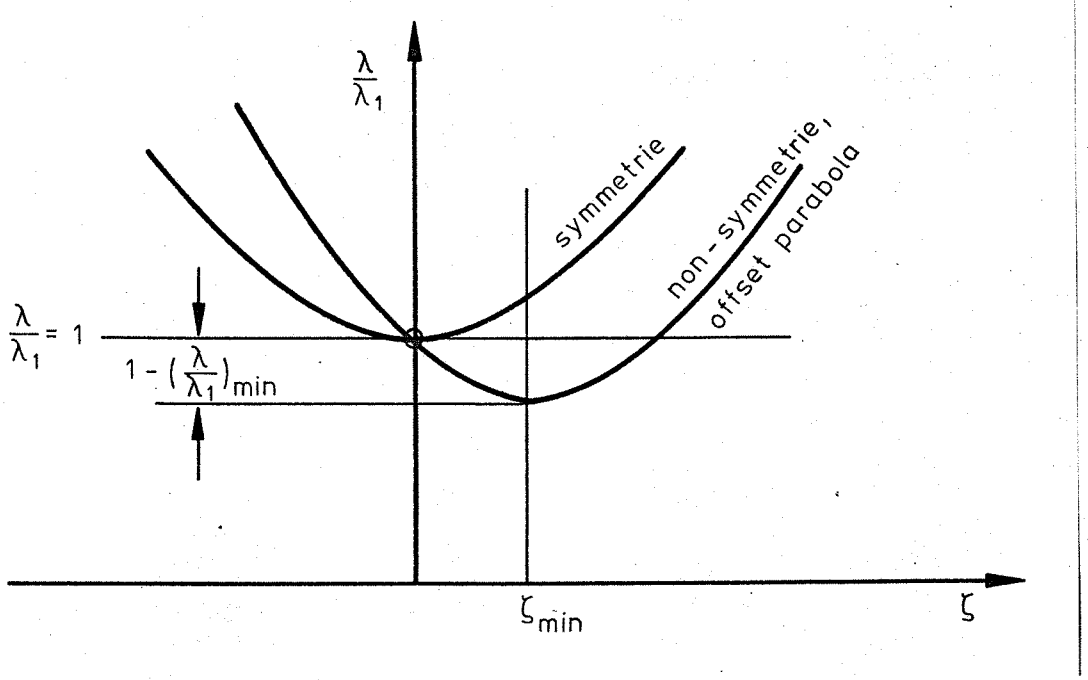

Finally the value K/K_o is given. For symmetrical bifurcation it represents the stiffness just after buckling. With non-symmetrical bifurcation the postbuckling line in the load-shortening diagram goes back along the fundamental line in the first instance, but

after some small amount of deflection it might also tend to assume the slope K/K_o. Due to the asymptotic nature of the theory, characterizing the initial postbuckling behaviour by the offset of the parabola λ/λ_1 vs. ζ and by the postbuckling stiffness, is justified only in cases of very small offset.

5. Comparison with Panel Tests

5.1 Description of Tests

The panels described in the preceding chapter were subjected to compression and shear in the test facility, Fig. 8. The test specimen forms part of the compression flange of a cantilever box beam. As such it is loaded in a similar manner a a panel in an airplane wing. The box beam is loaded at its tip. Bending by transverse tip displacement causes compression of the test specimen, twisting of the beam tip causes shear.

The stress distribution in the panel and the surrounding frame is statically indeterminate. It was necessary, therefore, to measure the load transferred by the panel. To either side 50 rosette strain gauges 0°/45°/90° were applied. Their readings taken at different load levels provided a good picture of the distribution of membrane forces in the panel. Moreover, by plotting corresponding stresses measured at opposite faces, see Fig. 8, the onset of buckling could be identified by a distinct deviation of these stresses.

5.2 Evaluation of Test Results

The membrane forces in the panel at the onset of buckling were determined from the measured strains by extrapolation. Defining this "onset of buckling" was somewhat arbitrary since the strains at opposite faces did not start to deviate suddenly. The membrane forces were used as input to the program BEOS which was run to compute eigenvalues and eigenmodes. The lowest eigenvalue λ_1 is the factor by which the distribution of membrane forces has to be applied in order to arrive at a theoretical buckling load. This factor should be slightly above unity for perfect

agreement between theory and test. An eigenvalue $\lambda_1 > 1.0$ means that the onset of buckling occurred below the theoretical buckling load. The program BOES also computed the characteristics of the initial postbuckling behaviour.

The axial membrane forces N_x in the center section of the panel were integrated along the panel width to yield the total axial force transferred through this section. It was plotted against the vertical beam tip displacement. This quantity is proportional to the shortening of the panel. Hence the plot may be considered as a load-"shortening" curve. The theoretical buckling load was indicated in the diagrams together with the theoretical slope in the initial postbuckling range.

Two tests with panel No. 3 and one test with each of the panels No. 4 and 5 were evaluated in this way, see Figs. 9 to 12. In the two tests with panel Nr. 3 different relations between compressive membrane forces N_x and shear flow N_{xy} were intentionally produced. In the second test the amount of shear was higher than in the first one. At the central point of the panel the relation between axial force and shear flow was

$$N_x / N_{xy} \approx 4 \quad \text{(panel No. 3, test No. 2)}$$

whereas

$$N_x / N_{xy} \approx 12$$

at test No. 1. At the tests performed with panels No. 4 and 5 this ratio was about

$$N_x / N_{xy} = 10.$$

Panel No. 3 could be tested several times although some small degradation of stiffnesses may have resulted from each test. For this reason the results of a third test were not included in this evaluation.

The panels No. 4 and 5 could be tested only once. Panel No. 4 attained a high load before buckles became visible. Shortly

later it buckled once more accompanied by a very loud report, and followed by partial debonding of face layers and core. The buckling behaviour of panel No. 5 was milder, but this panel was also destroyed after buckling.

In the diagrams, Figs. 9 to 12, the maximum loads can be seen clearly. They were divided by the theoretical buckling load. The rario N/N_x is given as written information in the diagrams. The onset of buckling is manifested by changes of slope on the load-shortening curves for panels No. 3 and 4, but not for Panel No. 5. All panels were able to carry additional loads. The tests were stopped with panel No. 3 in order to avoid destruction. The load carried by panel No. 4 decreased a small amount in the first instance, but increased again before the panel was destroyed. On panel No. 5 slight buckles grew visible but the load could be increased at the same rate as before until suddenly sharp buckles appeared, which caused delaminations.

Summarizing these results it may be stated that the initial post-buckling behaviour can be classified as "mild" for all panels. The panels with the greater curvature attained remarkably higher loads than the flatter one, but were destroyed, obviously in a secondary buckling process.

The theoretical results also predict "mild" initial postbuckling behaviour with stiffness degradation by 35% to 52%. The maximum loads attained were not lower than 77% of the theoretical buckling load. One test specimen, panel No. 4, could even be loaded to a value slightly above the theoretical buckling load.

6. References

[1] GEIER, B., KLEIN, H. — Stability Limits of Orthotropic Shallow Sandwich Shells - Computation and Test Results-. Proc. 11th Congress of the International Council of the Aeronautical Sciences 10-16 September 1978, Lisboa, Portugal, Vol. 1 ed. by J. Singer and R. Staufenbiel.

[2] KOITER, W.T. On the Stability of Elastic Equilibrium Translation of "Over de Stabiliteit van het elastisch evenwicht" Technische Hogeschool Delft, H.J. Paris, Publisher, Amsterdam, 1945, NASA TT F-10, 833, 1967, 202 pp.

[3] SEIDE, P. A Reexamination of Koiter's Theory of Initial Postbuckling Behaviour and Imperfection Sensitivity of Structures.

Symp. Thin Shell Structures, Calif. Inst. Technol., 1972 in "Thin-Shell-Structures" (Y.C. Fung, E.E. Sechler, eds.) pp. 59-80 Prentice-Hall, Englewood Cliffs, N.J., 1974.

[4] BUDIANSKY, B. Theory of Buckling and Post-Buckling Behaviour of Elastic Structures.

In "Adavances in Applied Mechanics" (edt. by Chia-Shun Yih) Vol. 14, 1974, pp 1-65.

[5] KOITER, W.T. Buckling and Post-Buckling Behaviour of a Cylindrical Panel under Axial Compression.

NLL Rep. 5476, 1956.

[6] POPE, G.G. The Buckling Behaviour in Axial Compression of Slightly-Curved Panels, Including the Effect of Shear Deformability.

Int. J. Solids Structures, Vol.4, 1968, pp. 323-340.

[7] ROHWER, K. BEOS, Buckling Loads and Natural Vibrations of Eccentrically Orthotropic Shells.

to be published as DFVLR-Mitt.

[8] GEIER, B. Ermittlung der Eigenschwingungen flacher Sandwichschalen mit dem Programm BEOS. (Calculating the Natural Vibrations of Shallow Sandwich Shells Using the Program BEOS.

Z. Flugwiss. Vol. 21, 1973, No. 12, pp 454-465.

N_x/N_{xy}	Panel No.	Bifurcation loads	Bifurcation mode type	Postbuckling Behaviour $\bar{\alpha}_1$	$\bar{\alpha}_2$	ζ_{min}	$1-\left(\frac{\lambda}{\lambda_1}\right)_{min}$	K/K_0
100/0	3	0.8253	a,s	0	0.814	0	0	0.449
		0.9094	s,s					
		1.2022	a,a					
	4 and 5	1.1825	s,s	0.101	1.943	0.026	0.001	0.660
		1.3083	a,s					
		1.373	s,a					
100/10	3	0.8153	(a,s, modified)	0	0.833	0	0	0.455
		0.1913	(s,s, modified)					
		1.1913	(a,a, modified)					
	4 and 5	1.1572	(s,s, modified)	0.064	1.992	0.016	0.0005	0.666
		1.2184	(a,s, modified)					
		1.3911	(a,a, modified)					

TABLE 1 RESULTS OF COMPUTATION FOR TEST PANELS UNDER IDEALIZED LOADS

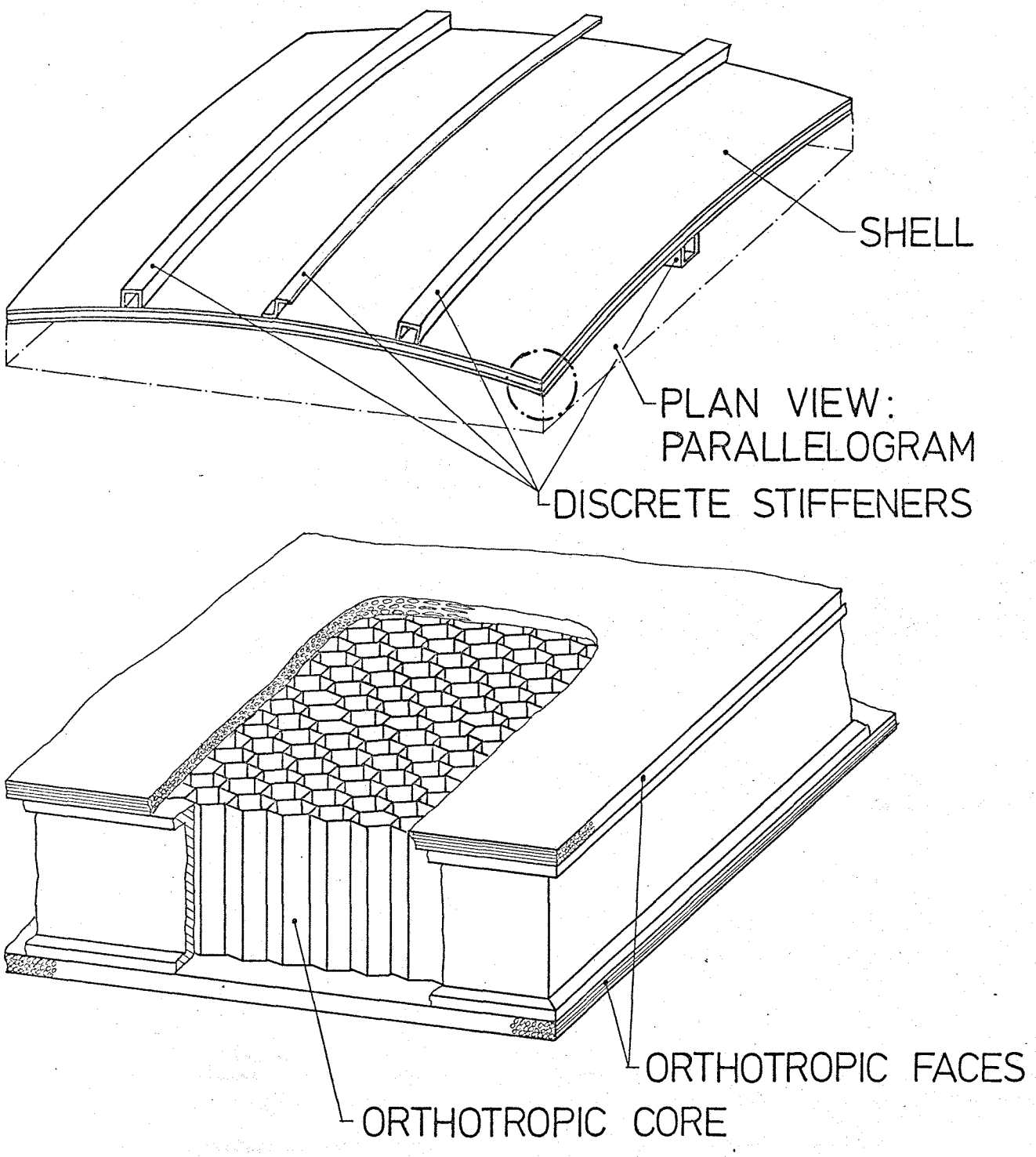

Fig. 1 SHELL CONFIGURATION FOR COMPUTER PROGRAMME BEOS.

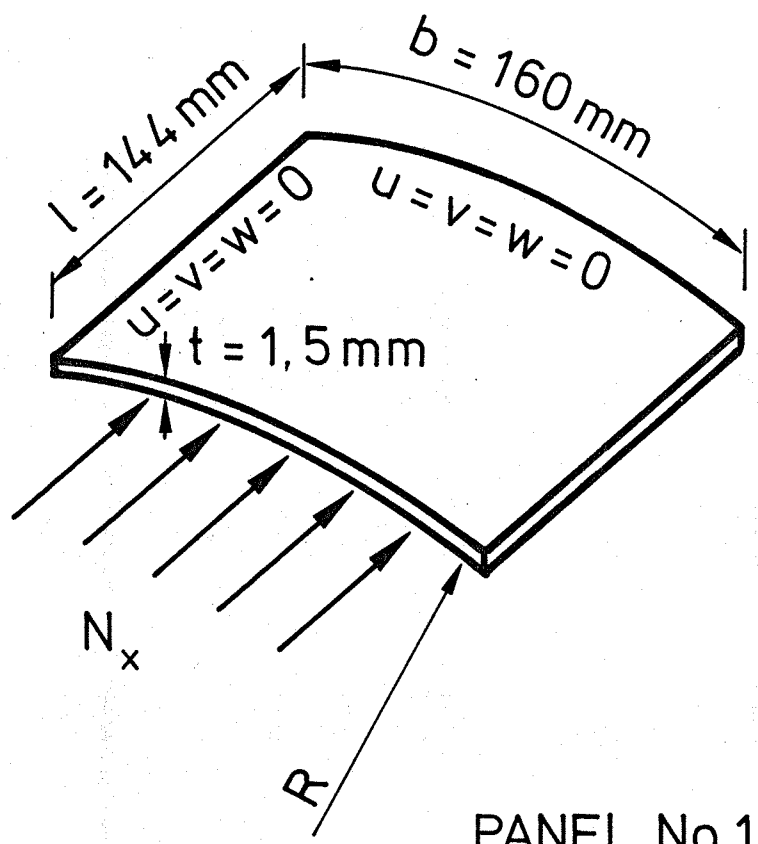

MATERIAL PROPERTIES :

$E = 71\,GPa$; $\nu = 0.3$

PANEL No.1: $r = 1000\,mm$; $\theta = \frac{\sqrt{12(1-\nu^2)}}{2\pi}\frac{b}{\sqrt{r\,t}} = 1.195$

PANEL No.2: $r = 831.4\,mm$; $\theta = 1.311$

Fig.2 ISOTROPIC PANELS , EXAMPLES FOR COMPUTATION

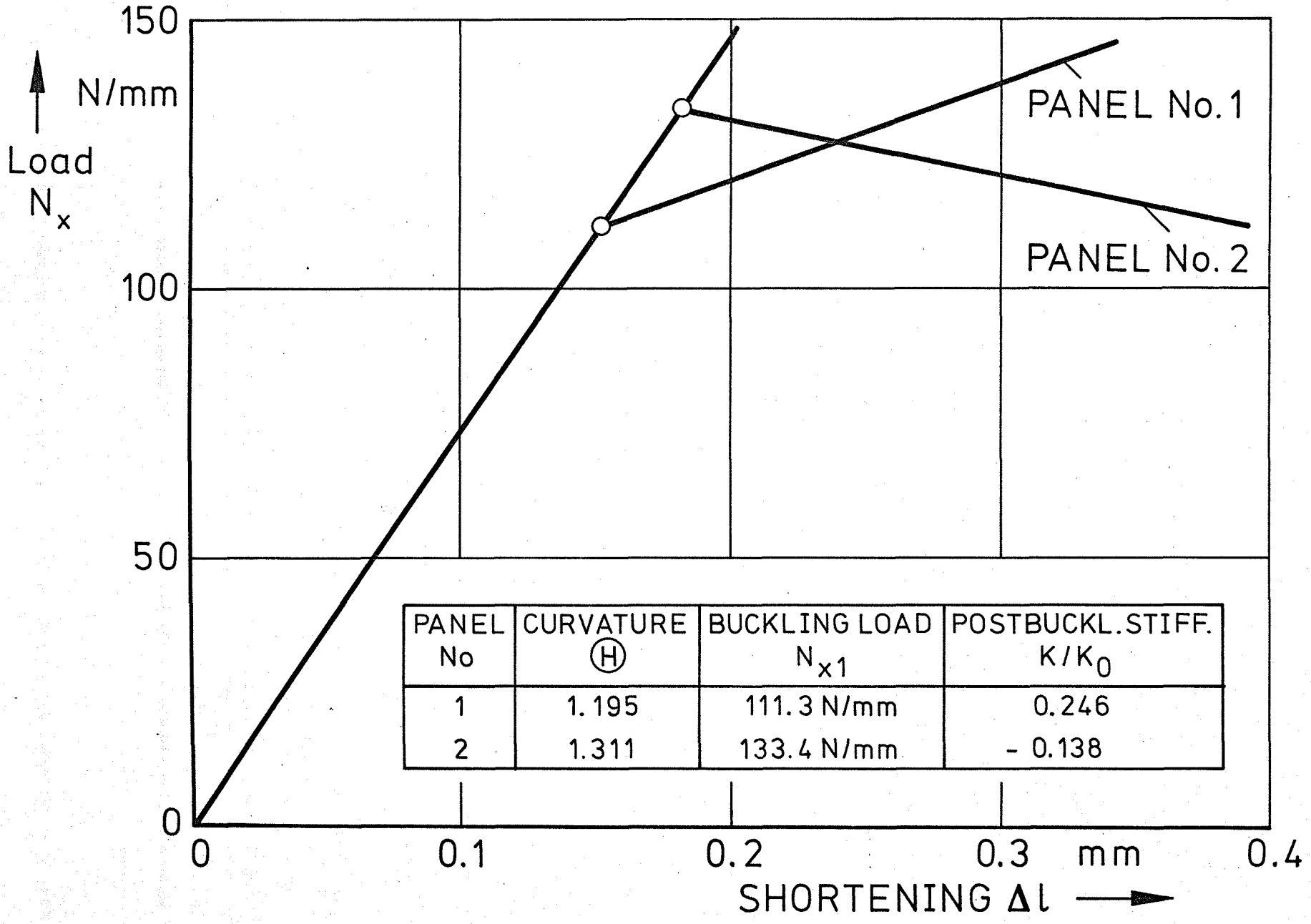

PANEL No	CURVATURE Ⓗ	BUCKLING LOAD N_{x1}	POSTBUCKL.STIFF. K/K_0
1	1.195	111.3 N/mm	0.246
2	1.311	133.4 N/mm	- 0.138

FIG. 3 ISOTROPIC PANELS, INITIAL POSTBUCKLING STIFFNESS

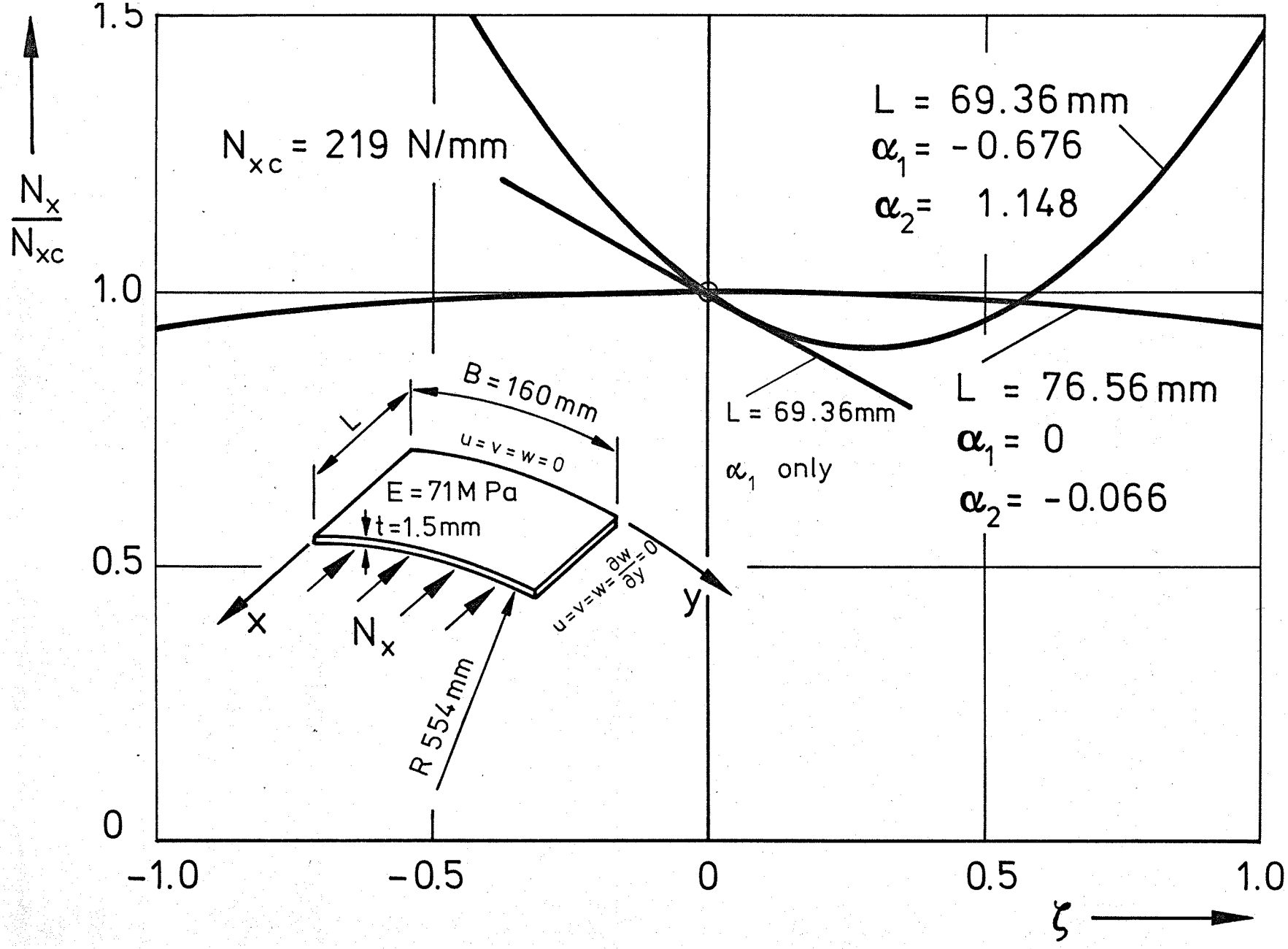

Fig.4 ISOTROPIC PANELS, LOAD-DEFLECTION DIAGRAM

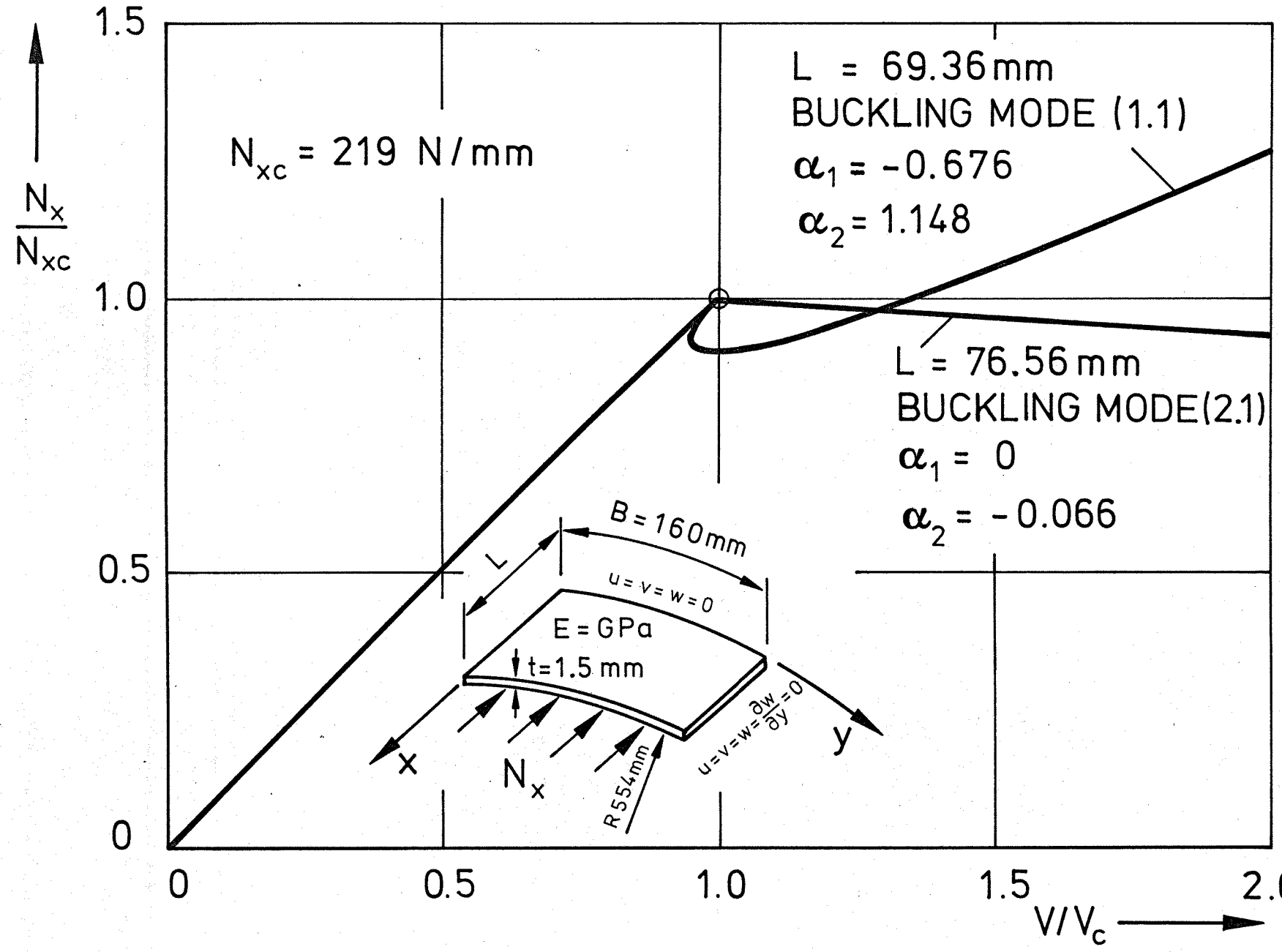

Fig.5 ISOTROPIC PANELS, LOAD - SHORTENING DIAGRAM

DFVLR152/GE0037

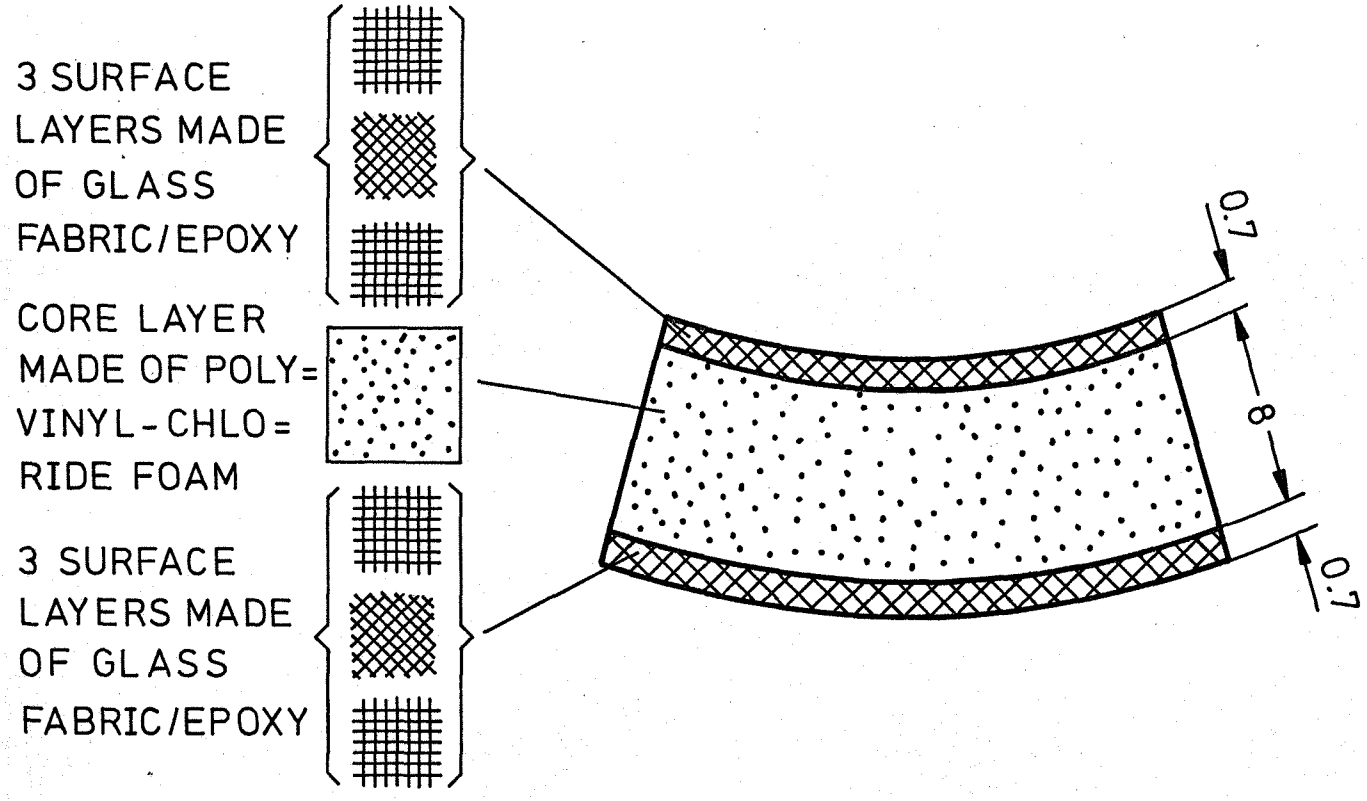

FIG.6 THE CONSTRUCTION OF THE PANEL

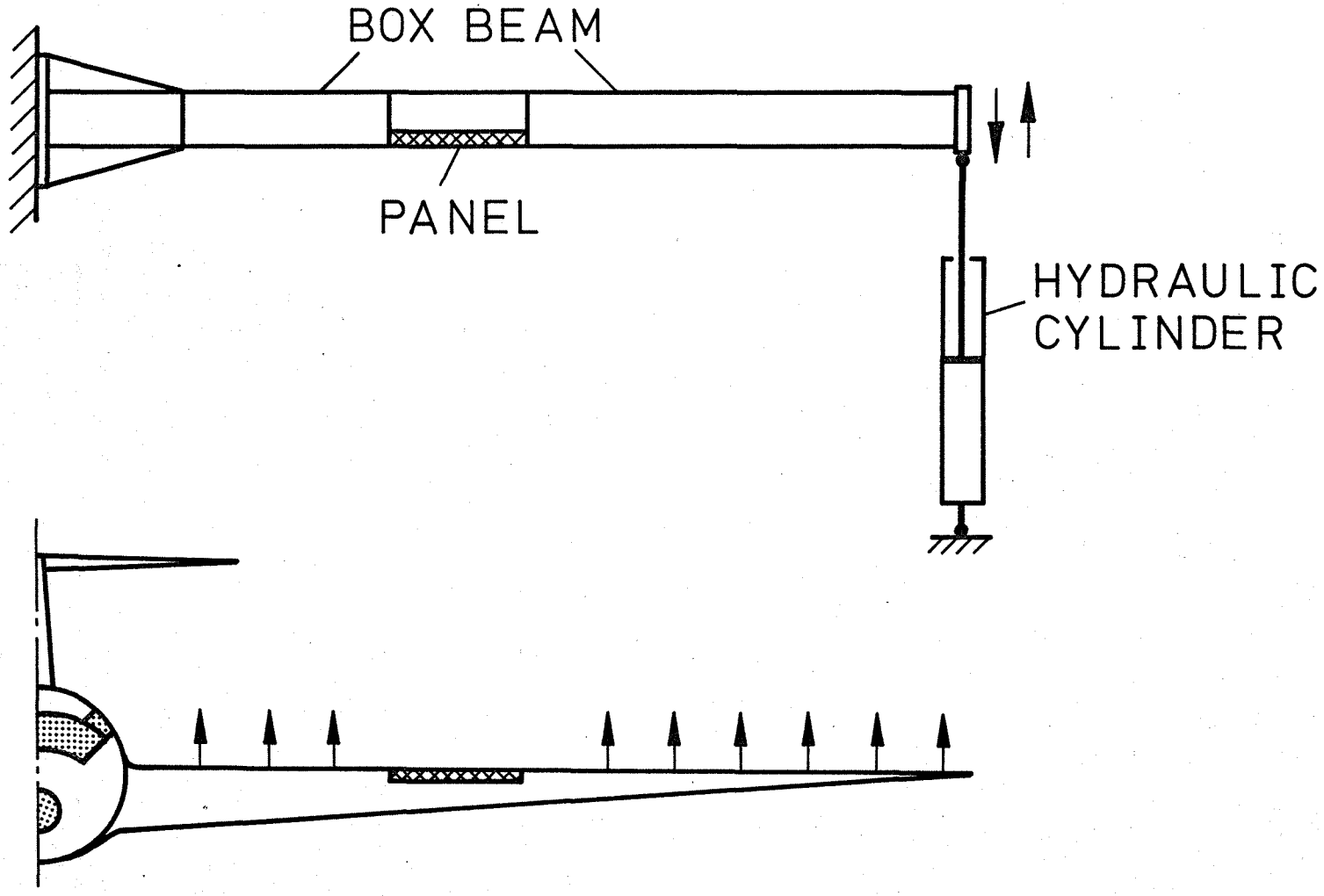

Fig.7 LOAD APPLICATION TO THE PANEL IN A WING AND IN THE TEST

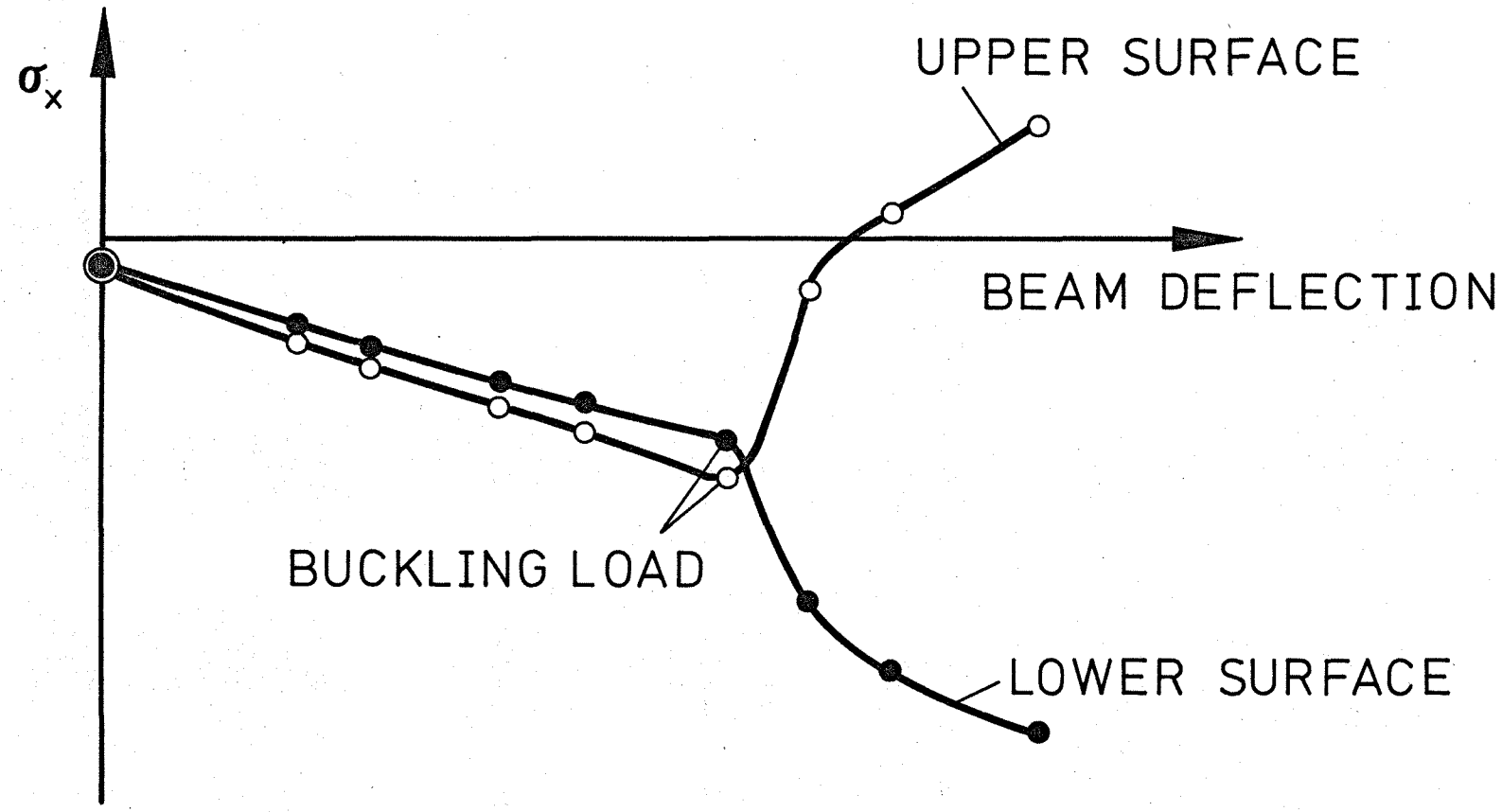

FIG.8 EXAMPLE OF CORRESPONDING STRESSES AT THE UPPER AND THE LOWER SURFACE

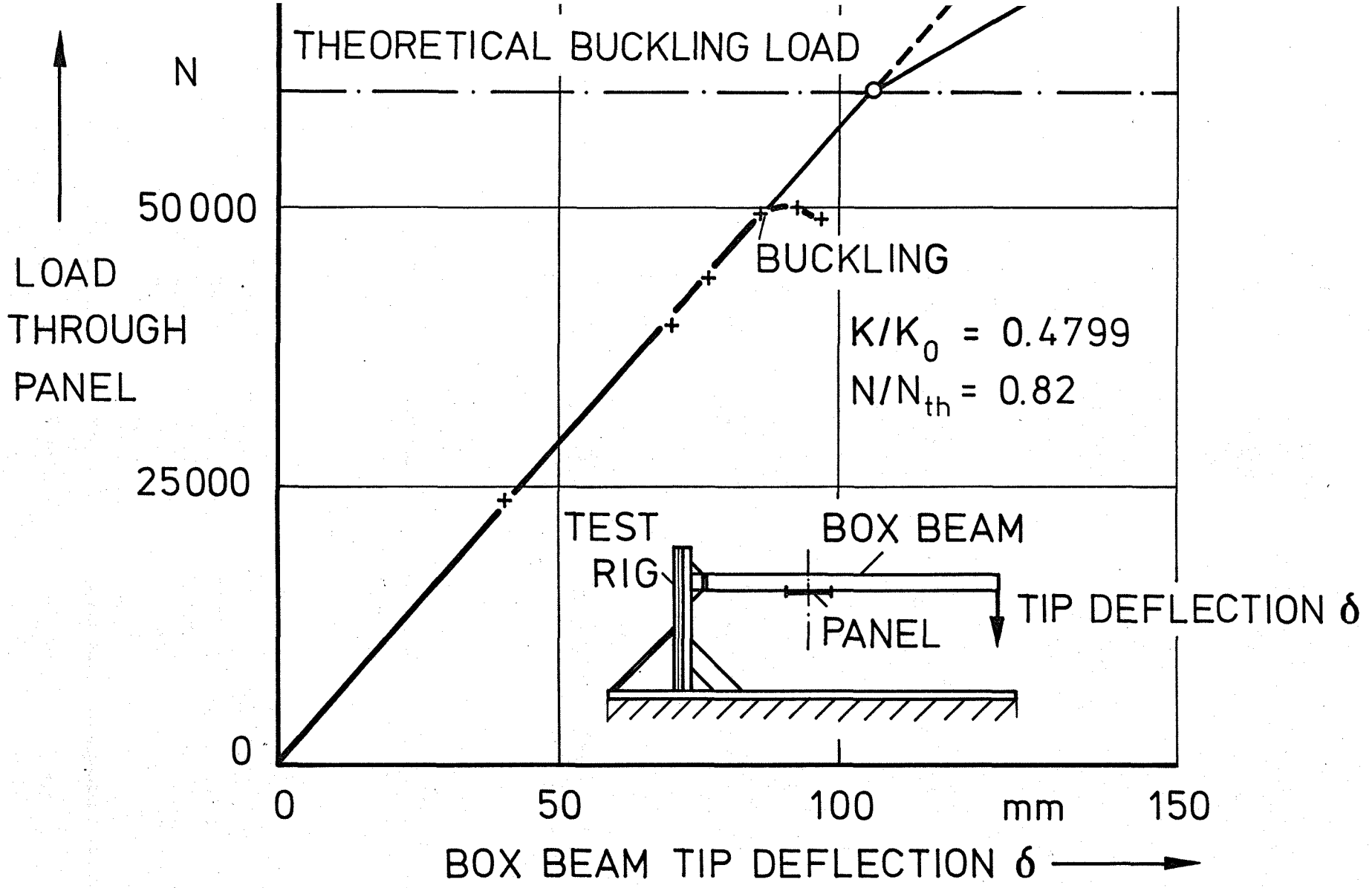

Fig. 9 RESULTS FOR PANEL No.3, TEST No.1

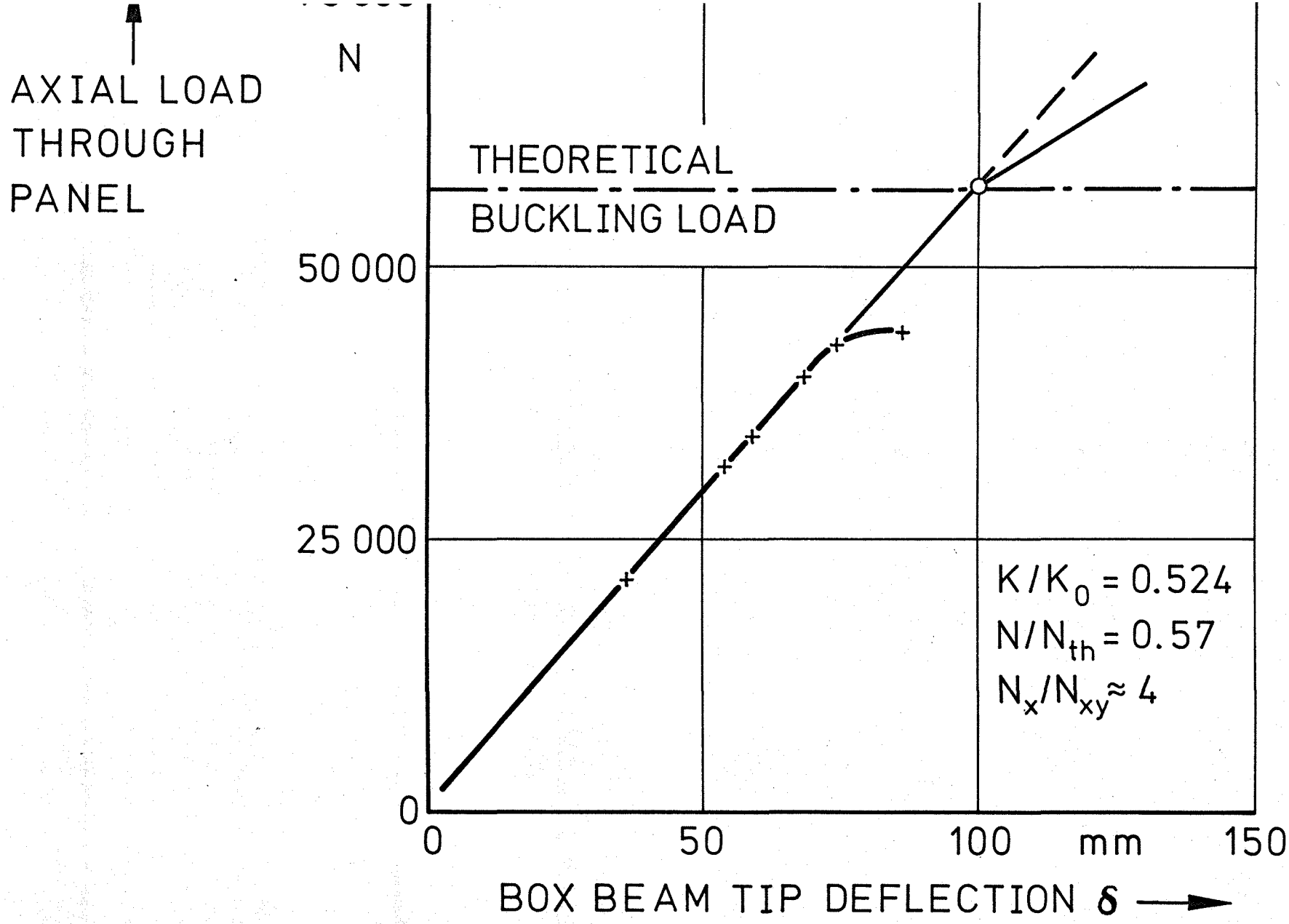

FIG.10 RESULTS FOR PANEL No.3, TEST No.2

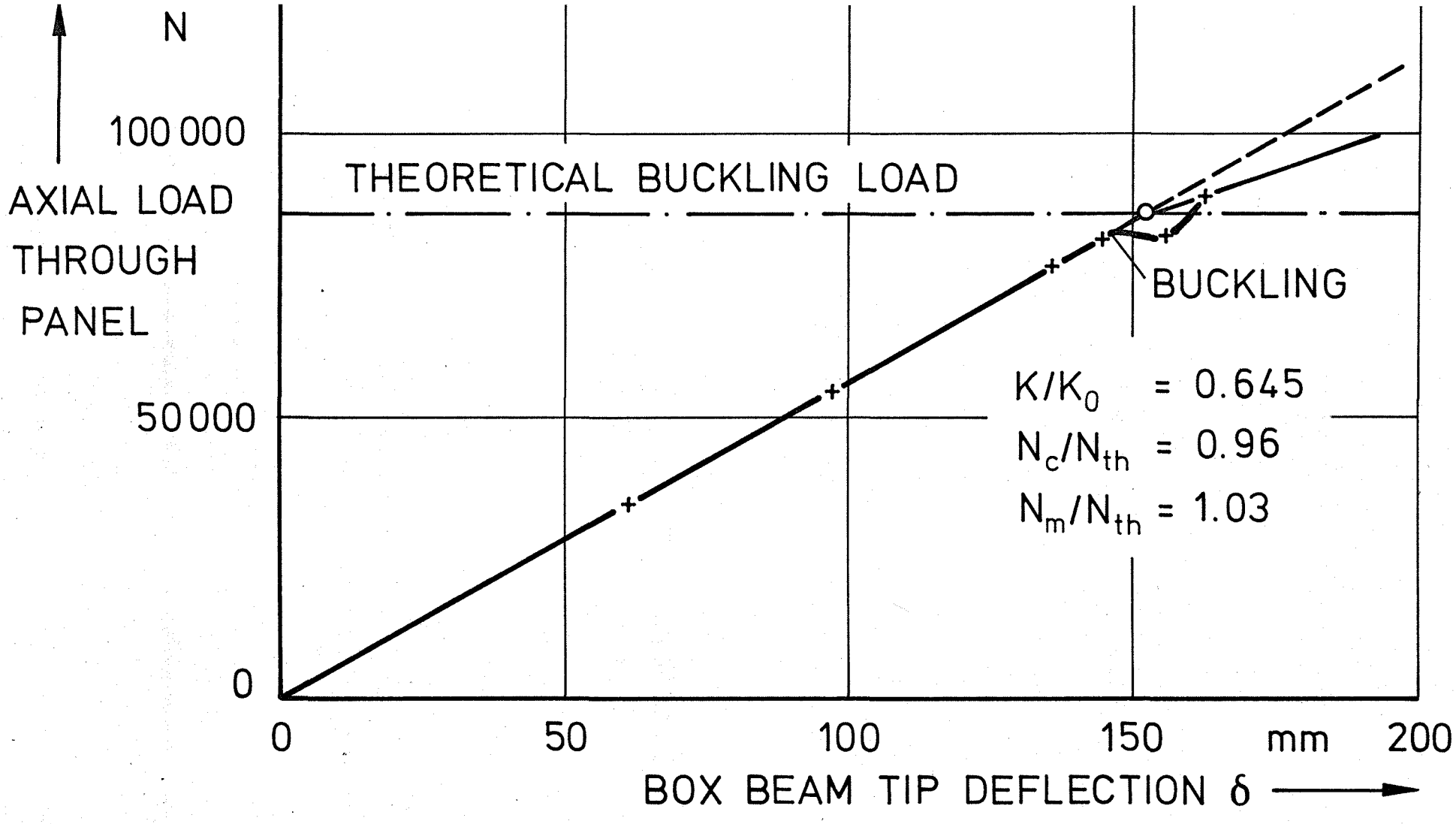

Fig.11 RESULTS FOR PANEL No.4

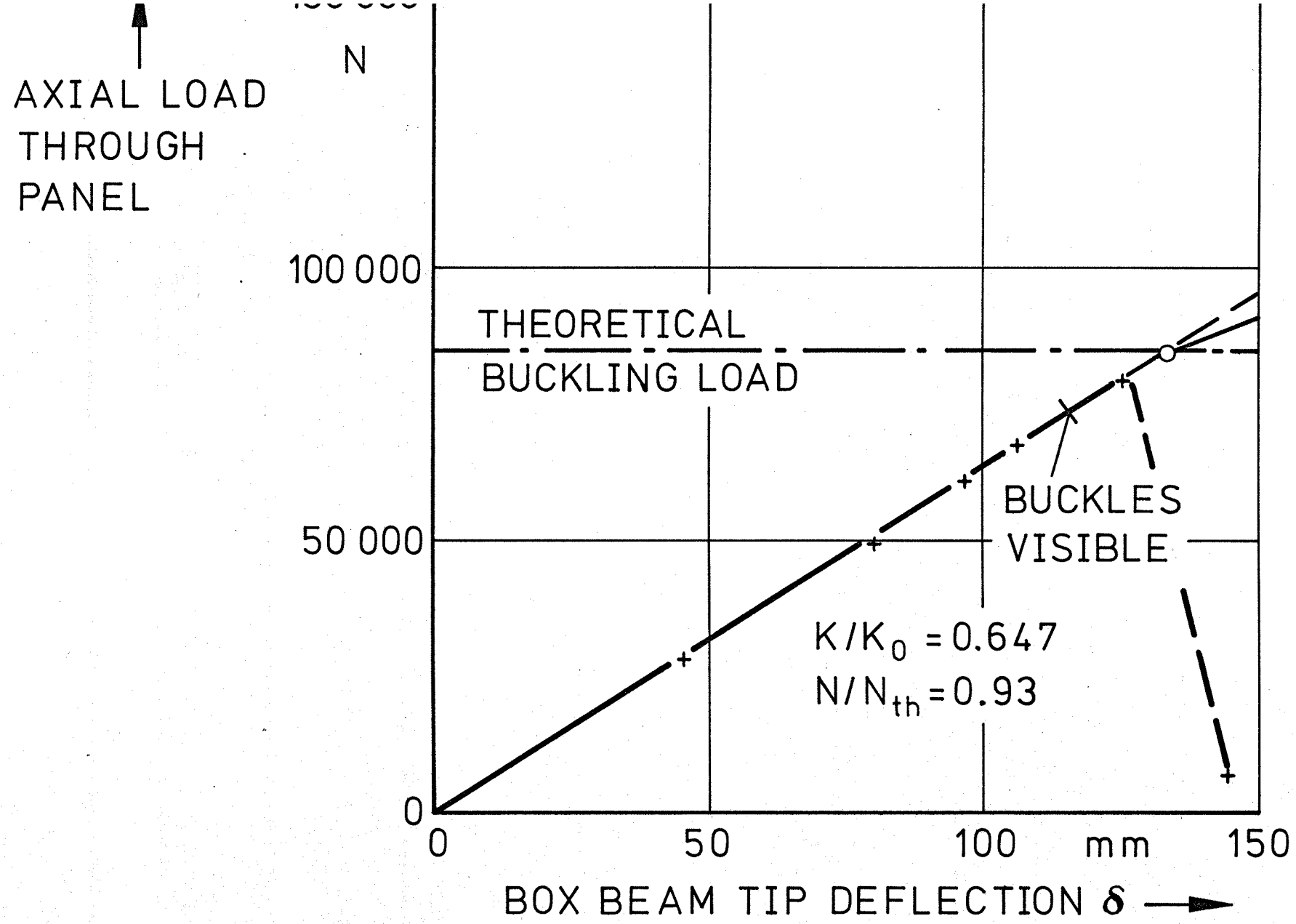

Fig. 12 RESULTS FOR PANEL No. 5

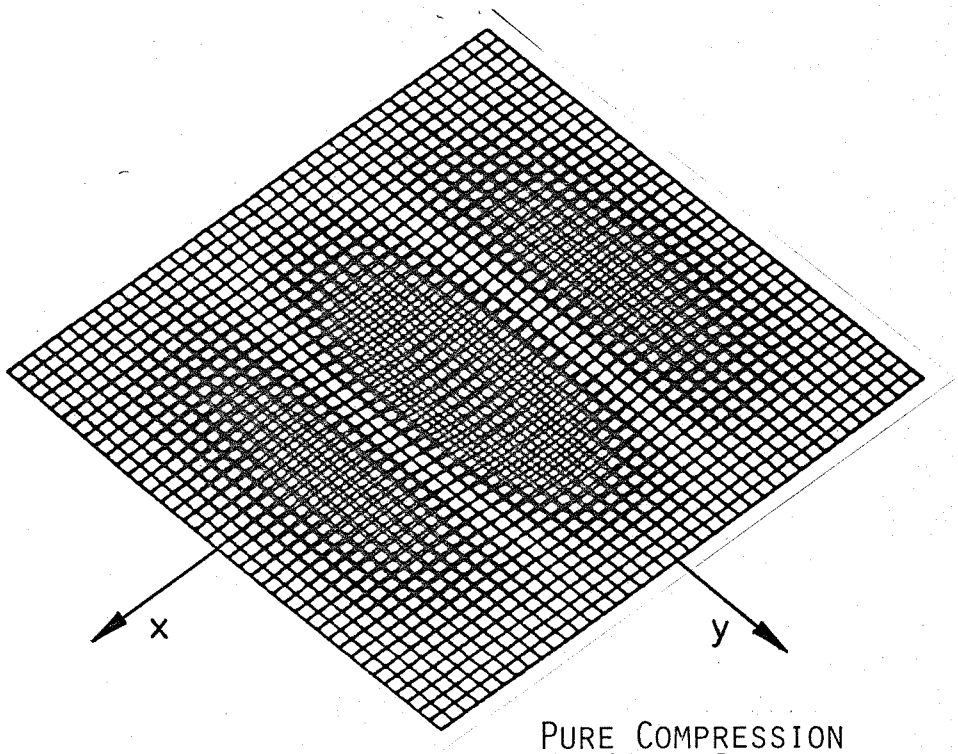

PURE COMPRESSION
$N_{XY}/N_Y = 0$

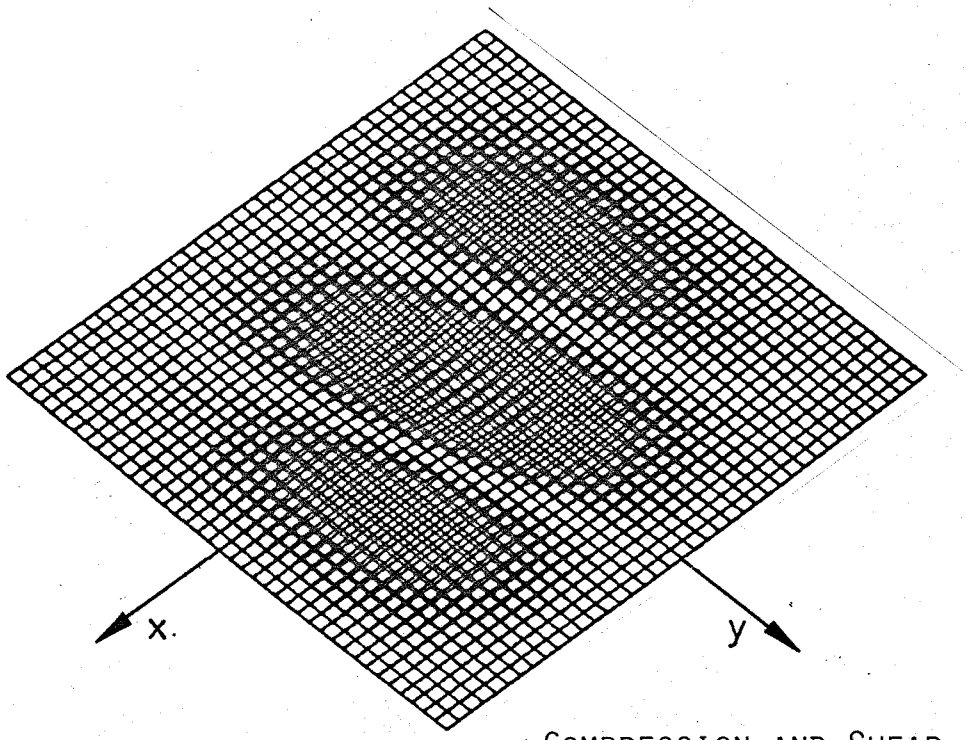

COMPRESSION AND SHEAR
$N_{XY}/N_X = 0.1$

FIG. 13 BUCKLING MODES OF PANELS NO. 4 AND 5